

Synergy of Analytical Approaches Enables a Robust Assessment of the Brazil Mystery Oil Spill

Christopher M. Reddy,* Robert K. Nelson, Ulrich M. Hanke, Xingqian Cui, Roger E. Summons, David L. Valentine, Ryan P. Rodgers, Martha L. Chacón-Patiño, Sydney F. Niles, Carlos E.P. Teixeira, Luis E.A. Bezerra, Rivelino M. Cavalcante, Marcelo O. Soares, André H.B. Oliveira, Helen K. White, Robert F. Swarthout, Karin L. Lemkau, and Jagoš R. Radović



Cite This: <https://doi.org/10.1021/acs.energyfuels.2c00656>



Read Online

ACCESS |



Metrics & More



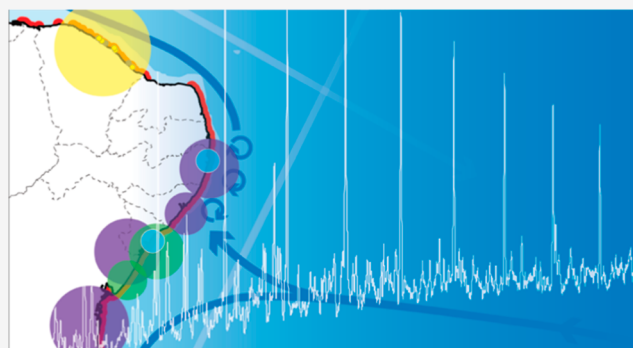
Article Recommendations



Supporting Information

ABSTRACT: From August 2019 to June 2021, viscous oil residues appeared along the Brazilian coast spanning 11 states and more than 3,000 km of tropical shoreline. Forensic results published to date indicate that the majority of oil samples collected share a common origin, yet the exact source of the mystery oil has yet to be conclusively determined. The proposed sources include illegal discharges from vessels traversing near, within, or downstream of Brazilian waters, leaking offshore platforms, natural seeps, and historic shipwrecks. To constrain the potential sources of oil and provide additional insights into the composition of the oil, we analyzed samples collected from the Ceará state coastal zone in 2019 with a broad suite of geochemical tools and approaches. These approaches included bulk elemental analyses and state-of-

the-art analytical platforms including comprehensive two-dimensional gas chromatography (GC × GC), gas chromatography with triple-quadrupole mass spectrometry, and Fourier transform ion cyclotron resonance mass spectrometry. Based on bulk and molecular features, field samples collected from northeast Brazil share the same source as other 2019 mystery oil samples collected over ~2400 km to the south. A shared source across the Brazilian coast points to an input location east of Brazil within the southern branch of the South Equatorial Current, allowing transport both north and south of the bifurcation. The relative abundance and composition of diagnostic markers were consistent with the published analyses of Venezuelan petroleum. The composition of the field samples is consistent with the blending of, at least, two different petroleum products, a common practice to produce an “on spec” product such as a fuel oil used to power an underway vessel. The two components appear to be the residuum from atmospheric distillation and a thermally altered, aromatics-rich, nondistilled material. To the best of our knowledge, no samples from potential sources are available for a direct comparison to field samples. Hence, these results play a supporting role in determining the source, and benefit efforts to understand short- and long-term weathering and recovery.



1. INTRODUCTION

Between late August 2019 and June 2021, a dark, viscous oil began washing ashore along the coastline of northeastern Brazil. Oil reappeared intermittently in 2020 and 2021 following periods of strong winds, high waves, and spring tides (Figure 1). The Bahia and Paraíba states' coastline was re-oiled as late as July 2021 and Rio Grande do Norte as late as June 2020.¹ The oil reached more than 55 coastal and marine protected areas² including the rich and diverse ecosystem of Abrolhos Marine National Park (Figure 1).^{3,4} Unique tropical marine ecosystems in the region, including intertidal sandstone reefs, rhodolith beds, sandy beaches, mangroves, estuaries, seagrass beds, and coral reefs, were all affected by the oil.^{5–7} With over 1000 oiled locations documented and more than 200 tons of oily material removed from impacted areas,⁸ this

event has been called the worst oil spill in the history of Brazil and the most extensive in the tropical coastal regions.²

The area impacted by the oil spill spans >3,200 km of coastline from the extreme northeast to southeast of Brazil covering 11 states (Figure 1).⁷ Examining the surface currents in the southwestern Atlantic Ocean indicates that the release likely occurred within the southern branch of the South Equatorial Current (sSEC) or in the waters close to its bifurcation and was subsequently carried northward and southward by the western boundary currents (Figure 1).⁹ Oil was transported north and then west along the continental slope by the North Brazil Current and south along the

Received: March 7, 2022

Revised: June 24, 2022

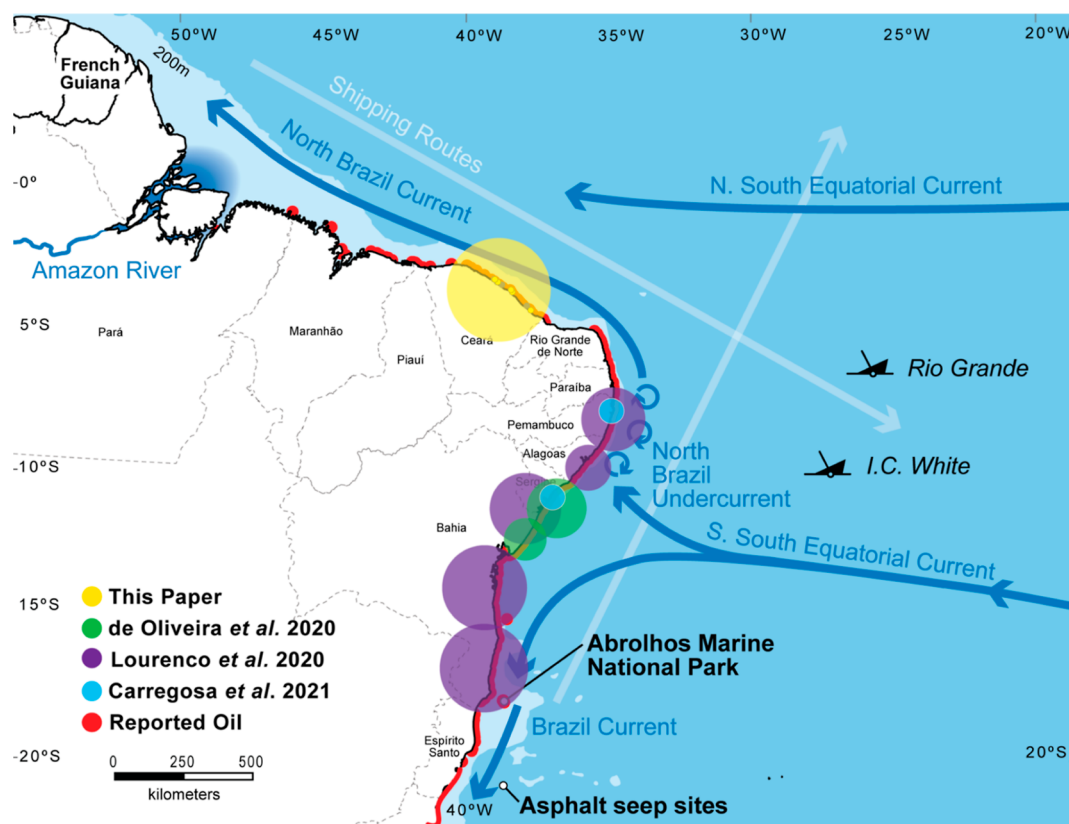


Figure 1. Map of Brazilian coastline with locations of reported oiling (red line) and field samples from this study (yellow circle), de Oliveira et al., 2020 (green circles),⁸ Lourenço et al., 2020 (purple circles),¹⁰ and Carregosa et al., 2021 (blue circles).¹¹ See Figure S1 and Table S1 for additional details on the locations and analyses performed on each sample in this study.

continental slope by the Brazil Current. From the continental slope, oil was moved toward the coast by cross-shore wind-driven circulation and tidal currents.⁹

Initial geochemical analyses of oil samples by gas chromatography with flame ionization detection (GC-FID) and mass spectrometry (GC-MS) indicated a common source.^{8,10} In addition, the spilled oil appeared to be crude oil or heavy fuel oil, with the origin consistent with a Venezuelan crude oil.⁸ Evaluation of hopane and sterane biomarkers present in the mystery oil by GC with triple-quadrupole MS (GC-QQQ-MS) supported these findings and suggested the oil was most strongly correlated with the oil from the Venezuelan Eastern basin.¹¹ Despite these efforts, the specific identity of the source of the spill remains a mystery with several hypotheses offered.^{7,12} The proposed sources include several wrecks in the region, particularly vessels sunk during World War II,¹³ an extraction platform (e.g., presalt or postsalt oil fields), or natural oil seeps (Figure 1). The primary hypothesis, however, was the oil originated from an offshore vessel that illegally dumped (intentional discharge) or accidentally released crude oil or a refined petroleum product.¹⁴ It is also possible that if the release occurred from an underway vessel, it may have carried¹⁵ and subsequently spilled multiple distinct fuels.^{16,17}

Several vessels were initially identified by Brazilian authorities as possible suspects responsible for the release. On November 1, 2019, the Brazilian government accused a Greek-flagged ship, the *Bouboulina*, of releasing crude oil approximately 700 km offshore in August 2019.¹⁴ It was then reported on November 6, 2019 that the Brazilian government

had added four more Greek-flagged oil tankers as suspects: *Maran Apollo*, *Maran Libra*, *Minerva Alexandra*, and *Cap Pembroke*.¹⁸ Another report by the Federal University of Alagoas released on November 17, 2019 pointed to another (as yet unnamed) vessel.¹⁹ More recently, Brazilian Federal police reaffirmed its accusation and concluded the *Bouboulina* was the source based on the ship's course and location, satellite imagery, and modeling/simulations of ocean currents.²⁰ In a separate investigation, the Brazilian navy determined the source was the *Bouboulina*, which was known to have departed from the Venezuelan port José Terminal Sea Island in late July 2019.²⁰ A subsample of *Bouboulina*'s cargo was not collected and hence unavailable for a direct comparison to field samples.

This oil spill, hereafter referred to as the Brazil mystery oil spill, presents a challenge to both characterize the oil composition and identify its source as well as an opportunity to investigate short- and long-term weathering and recovery. Advanced chemical analysis can provide geochemical insights into the oil composition and any changes that may have occurred during the refining process and after the spill. For example, Peters et al.²¹ reported that hydrocracking of feedstock completely removed monoaromatic and triaromatic steroids, while some steranes and terpanes were generated in the resulting product. Further investigation of the chemical composition of the oil spilled will detail to what extent it contains forensically valuable industrial chemicals, such as additives for oil recovery²² or any overprint from the preferential removal or addition of petroleum fractions that may have occurred during refining or other postrecovery facilities.²³ It is important to identify forensically valuable

compounds present in the oil so that it can be distinguished from current and future petroleum contamination.

This study collected and analyzed 14 oil samples from the Ceará state coastal zone, one of the areas most impacted by the oil spill.⁷ Recognizing that heavier and more viscous oils contain a continuum of molecules that challenge any single analytical platform, we used a suite of methods to characterize the bulk, elemental, molecular, and isotopic composition of oil residues. In addition to conventional GC-based analytical techniques primarily used in the aforementioned studies on the spill, and GC-QQQ-MS used in one study, we expanded our analysis with comprehensive two-dimensional gas chromatography (GC×GC) and ultra-high-resolution Fourier transform ion cyclotron resonance mass spectrometry (FT-ICR MS). The combined application of GC×GC and FT-ICR MS has uncovered and provided previously unattainable insights on fingerprinting and weathering of oils following the M/V *Cosco Busan* (2007),²⁴ *Deepwater Horizon* (2010),^{25,26} *Kirby 27706* (2014),²⁷ and *Southern Star VII* (2014)²⁷ oil spills, chronic pollution from coal tar,²⁸ and petroleum formation.²⁹ The insights provided here have utility in constraining possible spill sources, oil type, and understanding this event in the context of previous and future studies of oil spills.

2. EXPERIMENTAL SECTION

Sample Collection and Approach. Fourteen samples were collected from September to October 2019 on beaches spanning ~200 km along the northeast State of Ceará in Brazil. The collection locations for each sample are listed in Table S1 and shown in Figures 1 and S1 along with the local currents, shipwrecks, area of oiling, natural seeps, and locations of other samples collected following the Brazil mystery oil spill.^{8,10,11} These locations were easily accessed from land and near populated areas. The samples were collected above the high-tide line, initially stored in precleaned aluminum foiled envelopes prior to being transferred to glass jars in the laboratory, and then refrigerated until sample analysis.

A multitiered approach was used for analyzing the samples. Every sample was solvent-extracted and analyzed by GC-FID and GC×GC-FID (methodological details provided in the Supporting Information). Subsamples of Samples 1, 5, 6, and 12 were extracted separately and analyzed by FT-ICR MS at the National High Magnetic Field Laboratory (NHMFL; Tallahassee, Florida). Samples 12 and 13 represent the northernmost extent of sampling within this and other published studies (Figures 1 and S1) and were nearly devoid of sand. Due to their similar characteristics and sample size requirements, Sample 12, or a combination of Samples 12 and 13 (50/50) (hereafter referred to as Sample 12/13), was selected for further analysis via a wider range of analytical platforms and laboratories including elemental analysis, GC×GC-HRT, and GC-QQQ-MS (Table S1).

Bulk Analysis. The solvent-extracted residue for Sample 12 was analyzed in triplicate for bulk carbon, hydrogen, nitrogen, sulfur, and oxygen by Midwest Microlab (Indianapolis, IN). The bulk stable carbon isotope ratio was measured on CO₂ following combustion in an elemental analyzer. The saturate, aromatic, resin, and asphaltene (SARA) contents were determined by thin layer-chromatography with flame ionization detection, TLC-FID.³⁰ High-temperature simulated distillation from C₅ to C₁₂₀ was performed on Sample 12/13 by Triton Analytics (Houston, TX) using the ASTM method D-7169.

GC-FID and GC-MS. Every sample was analyzed by GC-FID at Wood Hole Oceanographic Institution to visually inspect and gauge general features (see Supporting Information for additional details).³¹ Each chromatogram was compared to previously published GC-FID chromatograms collected in response to the Brazil mystery oil spill.^{8,10} Sample 12/13 was analyzed for saturated hydrocarbons (HCs), polycyclic aromatic hydrocarbons (PAHs), S-heteroaromatics, and select biomarkers by Alpha Analytical (Mansfield, MA) using United States Environmental Protection Agency (EPA) Method 8015

analysis (GC-FID; saturates) and a modified 8270D analysis (GC-MS; PAHs and biomarkers). The methods and performance details are provided by Stout (2016).³²

GC-QQQ-MS. The solvent extract for Sample 12 was additionally processed with activated copper to remove elemental sulfur and fractionated into nonpolar and polar fractions with silica gel chromatography.³³ The nonpolar fraction was analyzed on an Agilent gas chromatograph (GC, 7890B) coupled to an Agilent triple quadrupole MS system (QQQ, 7010A) operated in multiple reaction monitoring mode to analyze C₂₆–C₃₀ steranes, C₂₁–C₂₆ tricyclic terpanes, and C₂₇–C₃₅ triterpanes, together with saturated and aromatic carotenoids. The isolated saturated HC fraction was also analyzed by GC-MS in full-scan mode for biomarkers.

GC×GC Analyses. Details on GC×GC-FID (all samples) and GC×GC-HRT (Sample 12) analyses are described elsewhere.^{27,31} Chromatographic peaks were identified with pure standards or tentatively identified based on retention times in both dimensions, mass spectral matches (above 80% similarity; NIST/EPA/NIH 05 Mass Spectral Library), or mass spectral interpretation.³⁴ See the Supporting Information for complete methods.

FT-ICR MS Ultrahigh-Resolution Mass Spectrometry. Samples were extracted in toluene/tetrahydrofuran (THF)/methanol (2:2:1) and diluted to 1:40 (vol/vol) in heptane to precipitate the asphaltenes. Thus, each sample yielded a maltene (heptane-soluble) and an asphaltene (heptane-insoluble) fraction. The whole extracts were analyzed for Samples 1, 5, and 6 as well as the maltene and asphaltene fractions for Sample 12. The extracts and fractions were analyzed by (+/– ESI) and (+) APPI FT-ICR MS using 9.4 T FT-ICR MS at the NHMFL.³⁵

3. RESULTS AND DISCUSSION

The single most valuable common denominator to compare the composition of oil between different studies on the Brazil mystery oil spill is GC-FID chromatograms. However, as uncollected oil continues to persist in the environment and weather, the diagnostic features available in GC-FID chromatograms will diminish and higher resolution, molecular-level analyses will be needed for a continued study of this spill.³⁶ To this end, the goals of our work were threefold. First, we wanted to confirm our samples were consistent with others collected in response to the Brazil mystery oil spill. Secondly, we wanted to provide a detailed molecular level characterization for source identification and to direct future monitoring studies. Third, we wanted to provide forensic support to characterize the type of spilled petroleum and spiller. Our results are summarized here, with additional tables, chromatograms, mass spectra, and other results in the Supporting Information (Tables 1, S2–S6; Figures S2–S11).

Fourteen samples were collected in September and October 2019 along the coastline of the Brazilian state of Ceará (Figures 1 and S1, Table S1). Twelve of the samples appeared to be oil mixed with varying amounts of sand with a slight luster. Two samples were dull, solid residues and looked heavily weathered (Samples 2.1 and 6) (Figure S2). A visual comparison of GC-FID chromatograms (Figure 2) and further quantitative analysis indicates the latter two samples were different from the other samples and unlikely connected to the Brazil mystery oil spill. Additional information on the characteristics and diagnostic ratios for Samples 2.1 and 6 are shown in Tables S4 and S5 and Figures S3, S8, and S9. Given the uncertainty regarding the source of these samples, we limit our discussion to the 12 remaining samples determined to be related to the Brazil mystery oil spill. All samples were analyzed by GC-FID and GC×GC-FID, while GC-MS, GC×GC-HRT, GC-QQQ-MS, bulk analyses, and FT-ICR MS were performed on a subset of samples (Table

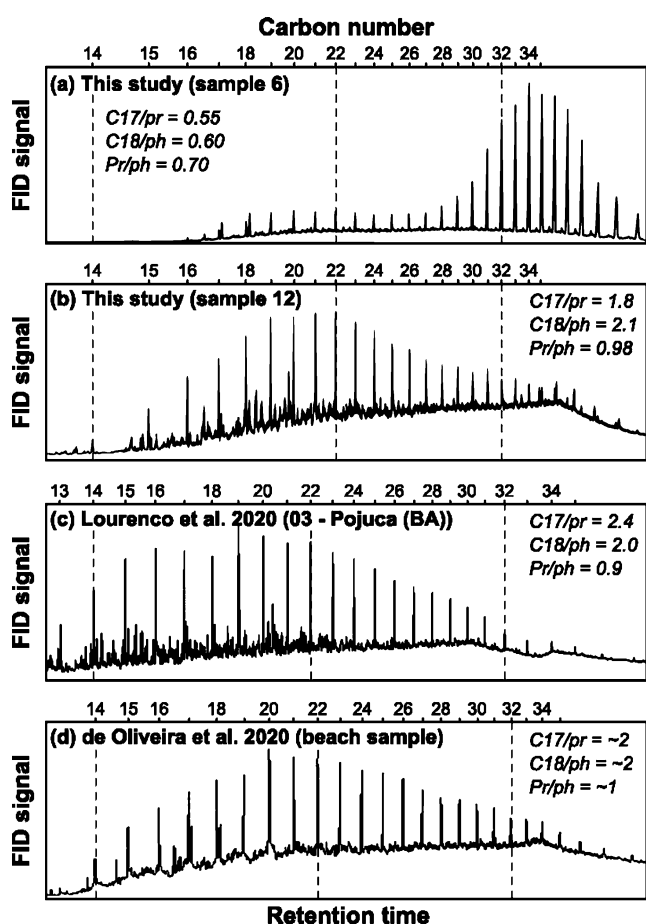


Figure 2. GC-FID chromatograms for (a, b) Stations #6 and #12 from this study, (c) Station #3 from Lourenço et al. (2020),¹⁰ and (d) beach sample from de Oliveira et al. (2020).⁸ (C) Reproduced with permission from ref 10. Copyright 2020 Elsevier. (D) Reproduced with permission from ref 8. Copyright 2020 Elsevier.

S1). Samples 12 and 13 represent the northernmost extent of sampling within this and other published studies (Figures 1 and S1) and were nearly devoid of sand.

Bulk Chemical Properties. The bulk properties of the material extracted from Sample 12 were consistent with a petroleum residue of a sulfur-rich source. Elemental analysis for carbon, hydrogen, nitrogen, and sulfur were 83, 10, 0.7, and 3.6%, respectively, with a molar C/H ratio of 0.7. The stable carbon isotope composition ($\delta^{13}\text{C}$) of the samples was -27.0% , consistent with the values reported by de Oliveira et al.⁸ The saturate, aromatic, resin, and asphaltene content was 9, 17, 49, and 25%, respectively, as determined by TLC-FID. The solubility in hexane and heptane was ~ 26 and $\sim 30\%$, respectively.

High-temperature simulated distillation (HTSD) of the extracted residue of Sample 12/13 yielded a cumulative mass of 10, 30, 50, 70, and 90% at the equivalent boiling points of C_{20} , C_{31} , C_{43} (approximate upper limit for GC-based techniques), C_{60} , and C_{108} , respectively (Figure S4).

These bulk measurements are consistent with a mixture of petroleum HCs with elevated amounts of polar, higher molecular weight non-GC-amenable components.

GC-FID Analysis of General Chromatographic Features and *n*-Alkanes. Analysis of the sample extracts by GC-FID showed a distribution of components across a carbon

number range of C_{13} to C_{41} (Figures 2 and S3). Normal alkanes and many other compounds were well resolved and rested upon a smooth and continuous unresolved complex mixture. GC-FID chromatograms did not exhibit a bimodal distribution, a feature that typically indicates mixtures of different petroleum types or mixing with background biogenic organic matter.^{37,38}

Quantitative analyses of Sample 12/13 by GC-FID determined that the total amount of *n*-alkanes and isoprenoids was 10 700 mg/kg (Figure 3 and Table S2). The ratio of resolved/unresolved HCs was $\sim 5\%$. The odd-over-even preference for C_{14} to C_{40} was 0.93. The C_{17} /pristane and C_{18} /phytane ratios were 1.8 and 2.1, respectively. The GC-amenable material from C_9 to C_{44} accounted for $\sim 25\%$ of the sample mass.

GC \times GC-FID analysis of Sample 12 yielded an ordered, three-dimensional chromatogram (Figure 4). Applying a signal-to-noise ratio cutoff of 500, a total of 2200 peaks were detected along a volatility basis in the first dimension (*x*-axis) and by relative polarizability in the second dimension (*y*-axis). Branched isoprenoids and *n*-alkanes eluted first in the second dimension and grouped along the *x*-axis (lower region of the chromatogram). More polar aromatic compounds were retained by the second dimension column and eluted later in the second dimension (see PAHs, top of the chromatogram). The sample contained an abundance of normal, branched, and cyclic alkanes between C_{14} – C_{41} , PAHs, sulfur-containing aromatics, and biomarkers (Figure 4). The chromatograms of the remaining 11 samples were similar (Figures S8 and S9).

Polycyclic Aromatic Hydrocarbons and Molecular Markers. The total amount of two- to six-ring PAHs for Sample 12/13 was 9900 mg/kg (Table S2; Figures 3 and S5) and comprised mainly of the parent and alkylated isomers of naphthalene, fluorene, phenanthrene/anthracene, fluoranthene/pyrene, and chrysene. Notably, there were detectable amounts of five- and six-ring PAHs, including benzo[*b*]fluoranthene, benzo[*a*]pyrene, benzo[*e*]pyrene, and benzo[*g,h,i*]perylene and their extended alkylated series (up to C_3 - and C_4 -homologues). The sum of the parent and alkylated S-containing heterocyclic benzothiophenes, dibenzothiophenes, and naphthobenzothiophenes was 180, 1900, and 1230 mg/kg, respectively (Figure 3; Table S2).

Alkylated PAHs were more abundant than the parent PAHs and exhibited a bell-shaped curve among the distribution, which is a typical feature of petrogenic sources (Figures 3 and S5).³⁹ Presumably, the spilled oil initially contained a full complement of naphthalene and benzothiophene and their alkylated homologues, and then abiotic weathering processes, such as evaporation and dissolution, preferentially removed naphthalene and C_1 -naphthalenes relative to the C_2 - to C_4 -naphthalenes. Similarly, the loss of lower molecular weight alkanes ($< \text{C}_{14}$) in the absence of extensive biodegradation (as demonstrated by the ratios of straight and branched alkanes) can also be attributed to abiotic weathering. Similar weathering changes in naphthalene and alkane compositions were observed within days to weeks following spills of fuel and crude oils.^{15,23}

Hopanes, diasteranes, steranes, and other molecular markers (Table S4) were present in all samples. Diagnostic ratios (Tables S5 and S6) and the chromatographic distributions (Figures 4–7) were consistent with a petroleum source and instructive on several fronts of this study. Future sections will discuss their application when comparing to other field

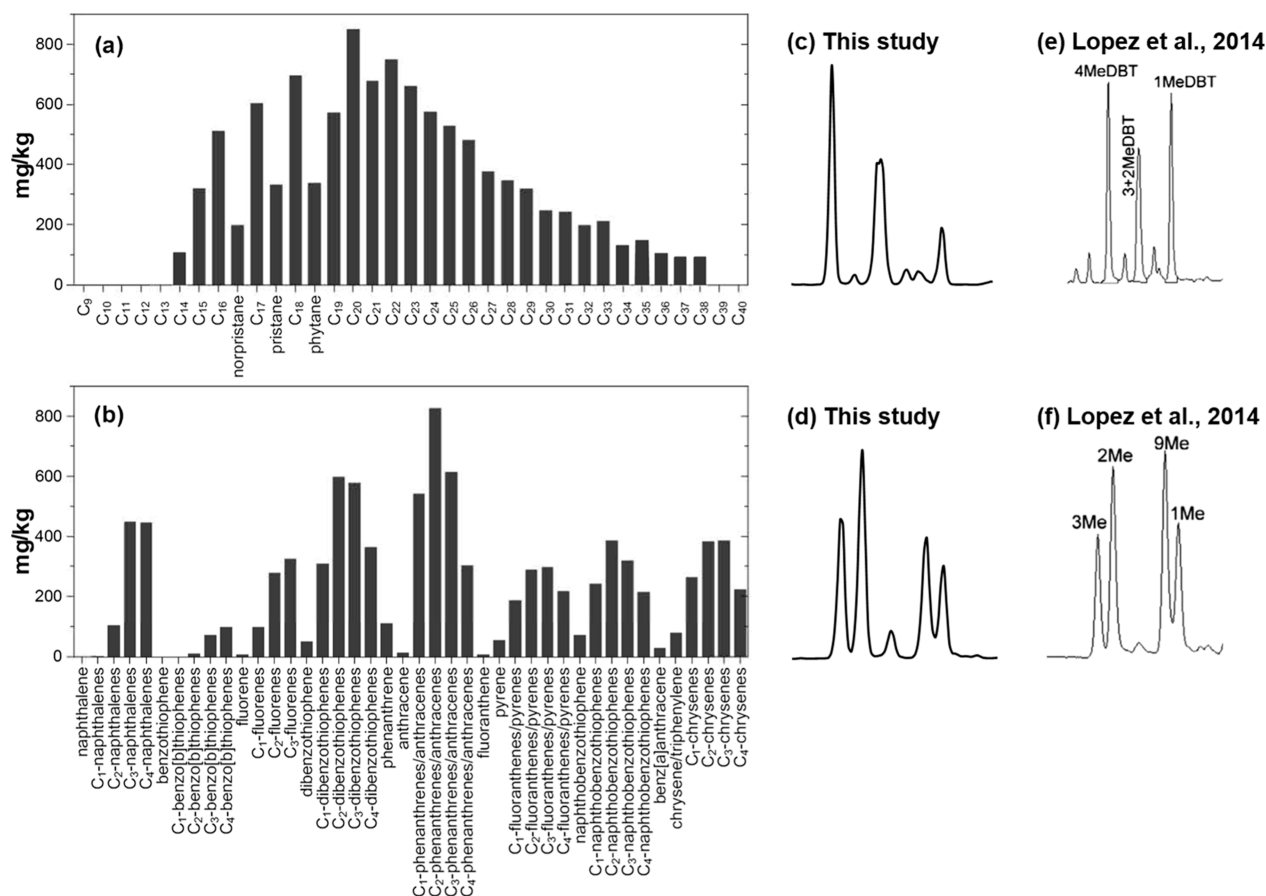


Figure 3. GC-MS analysis for Sample 12/13. (a) Saturates and (b) parent and alkylated PAHs. GC-MS-extracted ion current chromatograms: (c) m/z 184, C₁-dibenzothiophenes and (d) m/z 192, C₁-phenanthrenes/anthracenes for this study, (e) m/z 184, C₁-dibenzothiophenes and (f) m/z 192, C₁-phenanthrenes/anthracenes, reprinted from López, 2014.⁴⁷ Panels (e) and (f) are reprinted from *Organic Geochemistry*, 66, López, L., Study of the biodegradation levels of oils from the Orinoco Oil Belt (Junin area) using different biodegradation scales, Copyright (2014), with permission from Elsevier.

samples collected in 2019 along the Brazilian coastline, determining the geological origin and type of oil and utility for future studies.

Comparison to Previous Studies. Compared to previously published GC-FID chromatograms from samples collected in response to the 2019 Brazilian mystery oil spill, our 12 samples share features and similar C₁₇/pristane, C₁₈/phytane, and pristane/phytane (Pr/Ph) ratios (2, 2, 1) to those in the works of Lourenço et al. (2020)¹⁰ (2.4, 2.0, and 0.91) and de Oliveira et al. (2020)⁸ (2, 2, and 1), respectively (Figure 2). Notably, our samples appear to have lost more of the lower molecular weight compounds (Figure 2). Alternatively, different (and likely shorter) transport pathways and/or deposition mechanisms led to greater preservation of volatile compounds, as in the studies of Lourenço et al. (2020) and de Oliveira et al. (2020).^{8,10} For example, Lourenço et al. (2020)¹⁰ hypothesized that wax formation may have preserved their samples from extensive weathering.

Given the differences in GC-FID traces (Figure 2), we performed additional compositional analysis to determine if our samples shared the same source as those of Lourenço et al. (2020), Oliveira et al. (2020), and Carregosa et al. (2021).^{8,10,11} Quantitative analysis of diagnostic ratios supported the qualitative differences observed in GC-FID and GC×GC-FID chromatograms from Lourenço et al. (2020), Oliveira et al. (2020), and Carregosa et al. (2021)

(Figure 5).^{8,10,11} A comparison of overlapping diagnostic ratios in the aforementioned studies is listed in Table S4. An expanded list of ratios from GC×GC-FID revealed that our 12 samples were similar and had relative standard deviations of less than 10% for all but the oleanane/hopane (O/H) ratio, which had a relative standard deviation of 15%. The diagnostic ratios with the greatest variability were O/H, C₂₃ tricyclic terpane/17 α (H),21 β (H)-hopane (Tri-CT C₂₃H₄₂/H), 24-methyl-5 α (H),14 β (H),17 β (H)-20S-cholestane/17 α (H),21 β (H)-hopane (C₂₈ $\alpha\beta\beta$ -20S/H), regular C₂₇ steranes/regular C₂₉ steranes (C₂₇/C₂₉), and 24-methyl-5 α (H),14 β (H),17 β (H)-20R-cholestane/17 α (H),21 β (H)-hopane (C₂₈ $\alpha\beta\beta$ -20R/H) (Tables S4 and S5). Possible explanations are the presence of low amounts of, for example, oleanane, or preferential weathering for some sterane compounds.⁴⁰ The similarities between these diagnostic ratios, despite the differences in measurement methods, collection times, and locations, indicate that the three other studies also examined samples from the same unknown source.

Classification of Spilled Oil. Diagnostic molecules and ratios are often used to differentiate crude oils from petroleum products, especially fuel oils, that otherwise share similar GC-FID and GC-MS chromatograms.^{41,42} Prior studies have suggested this mystery oil may have originated as a Venezuelan crude.^{8,11} However, the isomer distributions of C₁-phenanthrenes/anthracenes and C₁-dibenzothiophenes indicate that

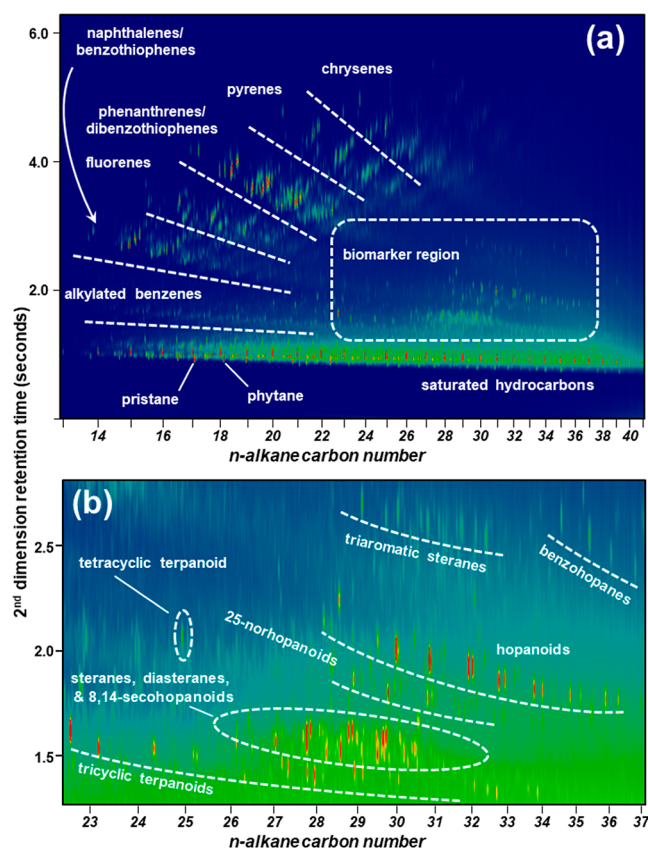


Figure 4. Annotated GC \times GC-FID chromatograms (plane view) for (a) full chromatogram and (b) dotted box in (a).

the mystery oil contains some thermally altered material. First, the more thermally stable 2- and 3-methylphenanthrene are preferentially enriched relative to 9/4- and 1-methylphenanthrene (Figure 3). Second, 2-methylanthracene was detected in our field samples (Figures 3, S5, and S7). This compound is not present or only present at trace levels in crude oils and petroleum distillates^{41,43} but has been found in numerous cracked products including coal tar, coal-tar-based asphalt sealant, creosote (coal), creosote (wood), byproducts of coal gasification, catalytic cracked gas oil, and fuel oils.⁴⁴ Third, the ratio of 2-methylanthracene to the total C₁-phenanthrenes/anthracenes was 0.05, within the range of 0.04 to 0.09 in modern heavy fuel oils that contain cracked materials ($n = 71$; Table S2).⁴¹ 2-Methylanthracene has also been found in fuel oils held in sunken vessels from the mid-20th century and in oils from numerous spills over the last several decades (Figure S7 and Table S5).¹³ Lastly, desulfurization and other thermal treatments of petroleum products preferentially enrich 4-methyldibenzothiophene relative to 2-/3- and 1-methyldibenzothiophene.^{44,45} The 2-/3- and 1-methyldibenzothiophene/4-methyldibenzothiophene ratio in our sample was 1.1 (Table S2) and greater than those measured in crude oils (Figures 3 and S5).⁴⁶ A comparison of our data with that of a Venezuelan crude oil highlights the aforementioned features indicating thermal alteration (Figure 3).⁴⁷ These findings signal that the Brazil mystery oil contains refined materials and not solely a virgin crude oil.

It is important to note that there is no set recipe for fuel oils. Sun et al. (2015)⁴² state that a fuel oil is a combustible product with a flashpoint greater than 37.8 °C. Others equate fuel oils as a blended mixture of a heavy refinery product (residuum)

with another lighter product (diluent). These differences were typified from the analysis of two spills of fuel oils that occurred in 2014.²⁷ The *Kirby 27706* spilled $\sim 760,000$ L of intermediate fuel oil in Galveston, TX, in March 2014. The *Southern Star VII* spilled $\sim 425,000$ L of a so-called “furnace oil” near the Sundarbans, Bangladesh. Furnace oils are confusingly another term for fuel oils. While both spilled oils were blended products that contained 2-methylanthracene, Chen et al. (2018)²⁷ concluded that the *Kirby* contained cracked residues that were at one point distilled while the furnace oil was prepared by blending a heavy crude oil with a cracked material that was not previously distilled.

Geologic Origin. Quantitative GC-MS analysis of Sample 12/13 contained a wide range of diagnostic compounds capable of constraining or identifying the geologic origin of the Brazil mystery oil (Table S3; Figures 3, 5, and 6) (GC-QQQ-MS analysis captured similar trends for hopanes, steranes, diasteranes, and triaromatic steroids but not presented). Briefly, the Brazil mystery oil is consistent with a source oil originating from marine organic matter deposited under anoxic conditions and a carbonate source rock. Pr/Ph ratios are one of the most widely used proxies for the assessment of redox conditions present during the oil source rock deposition. High Pr/Ph values (>3) are suggestive of terrestrial organic matter input under oxic conditions, and low values (<1) are indicative of anoxic conditions, while ratios in the range of 1–3 are characteristic of intermediate environments.⁴⁸ Pr/Ph ratios for our samples were 0.87 ± 0.07 (Table S5). Others have expanded the interpretation of this ratio to distinguish argillaceous source rocks deposited in a suboxic marine environment, from a carbonate anoxic marine environment.⁴⁹ An anoxic depositional environment is also supported by the dibenzothiophene/phenanthrene ratio <1 (0.45).⁵⁰ Distributions of regular steranes and triterpanes strongly support the marine or marginal marine (i.e., estuarine/deltaic) depositional environment and marine organic matter input, for example, C₂₇/C₂₉ sterane ratio is <1 , characteristic distribution of C₂₇, C₂₈, and C₂₉ steranes, high abundance of C₂₃ tricyclic terpane/hopane ~ 1 , and C₂₃ tricyclic terpane/C₂₄ tetracyclic terpane = 8.96)^{51,52} (Tables S4 and S5).

In addition, we attempted to further constrain the possible geological origin by a close inspection and comparison of the C₂₇–C₂₉ regular steranes relative to the published results for crude oils representative of the Venezuelan Eastern basin (Socororo field)⁵³ and Northwestern (NW) Lake Maracaibo basin (Caimbas field).³ When placed within the ternary plot of regular steranes, the representative samples from both basins fall within the compositional space that corroborates a Mesozoic marine origin,^{54,55} albeit with the distinguishable separation of the two basins, mainly driven by the content of C₂₇ and C₂₈ steranes (Figure 5). Hence, our samples appear to be compositionally more related to the NW Maracaibo basin samples. We report this observation as an incentive for further petroleum geochemistry studies of Venezuelan and other marginal South Atlantic basins that may help further constrain the origin of the Brazil mystery oil spill.

GC \times GC-FID analyses identified a suite of 8,14-secohopanes whose origin is still somewhat ambiguous in the literature, but they have been associated with biodegraded oils.⁵⁶ Another suite of biomarkers were the 25-norhopanoids, which have previously been detected in heavily biodegraded oil reservoirs (Figures 4 and 7).^{53,57} The possibility that the investigated residue contains some biodegraded oil is consistent with the

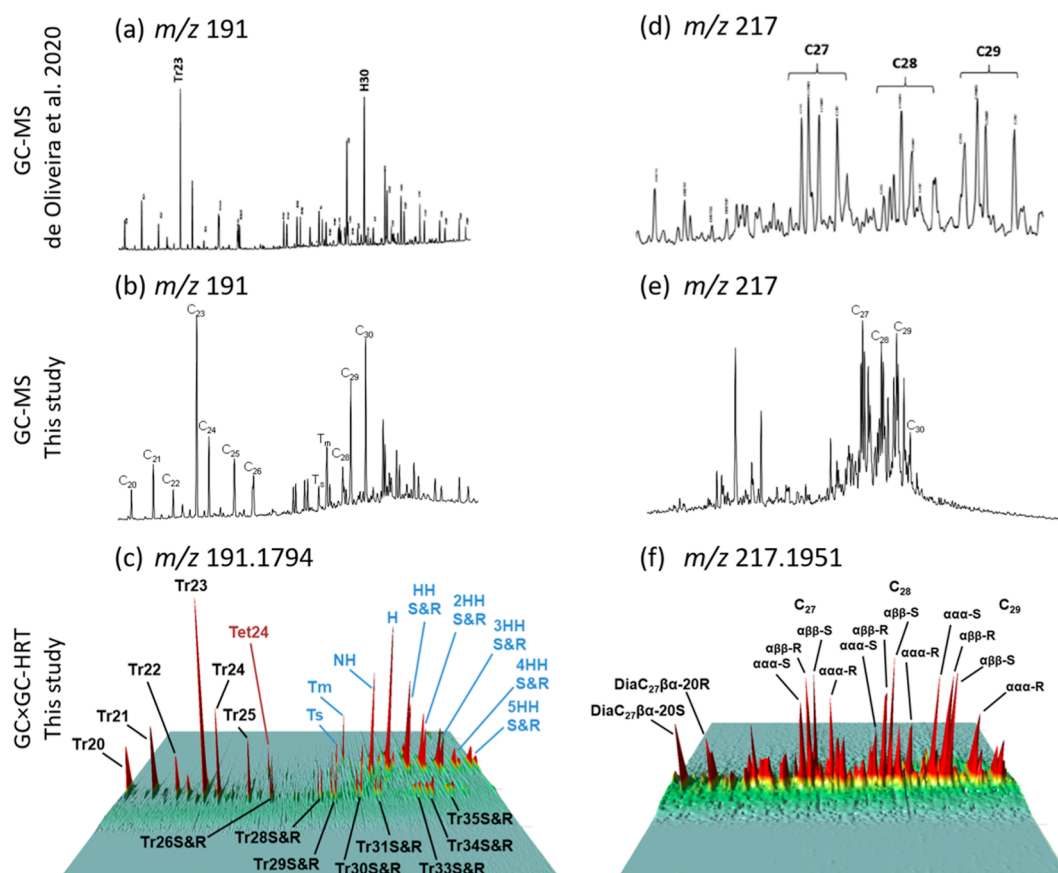


Figure 5. Extracted ion current chromatograms: (a,d) GC-MS m/z 191 and m/z 217, from de Oliveira et al. (2020);⁸ (b,e) GC-MS m/z 191 and m/z 217, from this study, and (c,f) GC × GC-HRT m/z 191.1794 and 217.1951. (a,b) Reprinted from *Marine Pollution Bulletin*, 160, de Oliveira, O. M. C., Queiroz, A. F. de S., Cerqueira, J. R., Soares, S. A. R., Garcia, K. S., Filho, A. P., Rosa, M. L. d. S., Suzart, C. M., Pinheiro, L. L., & Moreira, Í, T. A., Environmental disaster in the northeast coast of Brazil: Forensic geochemistry in the identification of the source of the oily material, *Copyright* (2020), with permission from Elsevier.

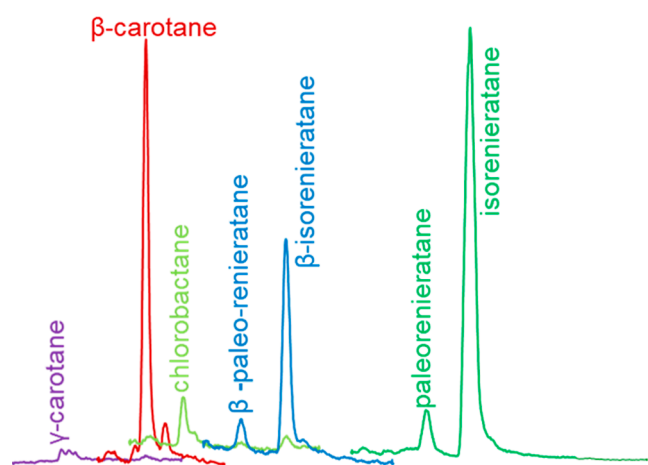


Figure 6. GC-QQQ-MS chromatogram of saturated and aromatic carotenoids in Sample 12.

observations from GC-MS, namely m/z 191 and m/z 217 traces, which are similar to the previously reported fingerprints of oil from Eastern Venezuelan basins^{53,58} as well as Lake Maracaibo Basin in northwestern Venezuela³ (Figure 5). A plausible hypothesis to reconcile this observation with apparent low biodegradation levels inferred from C_{17}/Pr and C_{18}/Ph ratios would result from the mixture(s) of oils of

different biodegradation levels, that is, lightly and heavily biodegraded.³

Archaeal core ether lipids (ACLs) including biphytane and ACL-3 were also detected by GC×GC.^{29,36,59} The high abundance of the three-ring phytane fragment could potentially be an indicator of planktonic marine archaea as well as another genetic marker of marine origin of the spilled oil.⁶⁰ These compounds are difficult to measure with one-dimensional GC. Yet, with GC×GC analysis, biphytane played a key role distinguishing the nearby naturally seeped oil and oil released during the 2015 Refugio pipeline spill (Goleta, CA).³⁶ While the “outlier” samples (2.1 and 6) are unlikely to represent the background signal of all inputs of petroleum HCs along the Brazilian coastline, the ACL-3/biphytane ratios in these two samples were the most different among the 12 samples. The structure of the ACLs points to recalcitrance, which in turn suggests that the ACL-3/biphytane ratio could be useful for tracking the residues from the 2019 Brazil mystery oil spill in the future, as other, less recalcitrant diagnostic compounds become less forensically useful.

An appreciable abundance of nontypical sterane diginane, which has been related to increased thermal maturity,⁶¹ was also observed. Diginane has been reported previously in some marginal South Atlantic oils.⁶² GC×GC-HRT was also used to confirm the identity of biomarkers (Figure 7) and record the mass spectra for 34 biomarkers (see Appendix 1 in the Supporting Information).

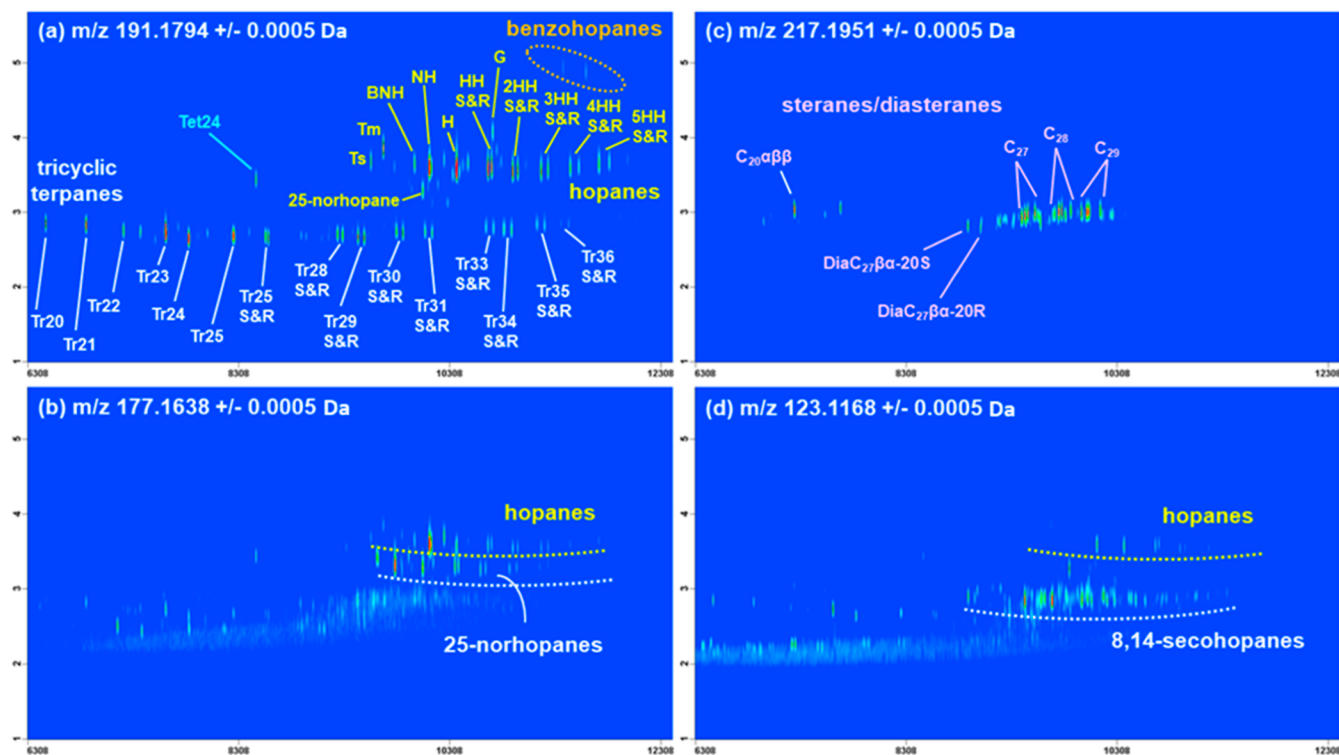


Figure 7. Plane view GC \times GC HRT-MS extracted ion current chromatograms for (a) m/z 191.1794, (b) m/z 177.1638, (c) m/z 217.1951, and (d) m/z 123.1168.

The diagnostic ratio of oleanane/hopane was below 0.1 (0.08), indicating that the age of the rock sourcing the analyzed oil is early-to-late Cretaceous,⁶³ which was further supported by C_{26} sterane distribution (Figures 4, 5, and 7). Oils from younger source rocks, that is, Cenozoic, would contain a higher abundance of both oleanane and 24-norcholestanes.⁶⁴ While de Oliveira et al.,⁸ did not detect oleanane, Carregosa et al.¹¹ reported oleanane/(oleanane + hopane) ratios of 0.06, 0.13, 0.15, and 0.16 for their four samples (0.13 ± 0.05). In this study, for all 12 samples, the oleanane/(oleanane + hopane) ratios were 0.07 ± 0.01 (Table S4).

Additional insights into the geologic origin of the Brazil mystery oil were uncovered from the analysis of carotenoid-derived HCs via GC-QQQ-MS analysis.³³ While not previously employed for oil spill forensics, this class of biomarkers captures the upper ocean conditions of primary productivity (e.g., light availability, taxa, and oxygenation) and depositional environment, which in turn helps characterize the source organic matter for petroleum generation.⁶⁵ Sample 12 contained an abundance of β -carotene, isorenieratene, and paleorenieratene and lesser amounts of β -renieratene and β -paleorenieratene (Figure 6). Little or no reneirapurpanane, reneiratane, and degradation products were detected. This signature is associated with low light-adapted, brown-pigmented strains of green sulfur bacteria in the photic zone and burial in low-oxygen, sulfidic depositional environments, that is, euxinia. Generally speaking, lacustrine settings are commonly lean in sulfide, whereas marine settings are relatively stable in sulfate supply.⁶⁶ Therefore, sulfidic water columns are typical to marine settings that are either permanently stratified or subject to strong upwelling cycles that bring deep sulfide-bearing waters into the photic zone.^{67,68} Collectively, the distribution of carotenoid-derived HCs in the

Brazil mystery oil supports an organic matter with a marine origin.^{66,69}

In summary, the indicators of organic matter source and depositional history for the mystery oil samples are consistent with the marginal South Atlantic basins in Colombia, Venezuela, and Brazil.^{70–72} Similar basins are also present along the conjugate margin along the Western African coast from Ivory Coast to Angola.⁷² However, oils from some of the Western African basins, for example, in the Niger Delta, have high Pr/Ph ratios (in the ~ 2 – 3 range) associated with a significant input of terrestrial organic matter to the depositional environment.⁷³

Synthesis of GC-Based Analyses. Traditional and advanced GC-based analyses of field samples collected in September and October 2019 agree on the overall characteristics of the Brazil mystery oil (Table 1) and are consistent with previously published peer-reviewed research works.^{8,10}

High-temperature GC-FID (simulated distillation) revealed a wide carbon range and appreciable amounts of non-GC-amenable material. GC-FID and GC \times GC-FID also showed a wide carbon range and unimodal distribution of HCs including *n*- and branched alkanes. Evaporation appears to have resulted in the loss of some HCs $< C_{15}$. Biodegradation may have occurred, but this loss was not extensive based on the continued presence of *n*-alkanes. The relative abundance and composition of PAHs analyzed by GC-MS were dominated by a petrogenic signal. However, the presence of five- and six-ringed PAHs and 2-methylanthracene indicates some or all the petroleum was thermally altered. Diagnostic molecules (biomarkers) from the analysis by GC-MS, GC \times GC-FID, and GC-QQQ-MS are consistent with the marginal South Atlantic origin, likely Venezuelan, and possibly from Western Venezuela. GC \times GC-HRT analyses identified both 25-norhopanoids and 8,14-secohopanes. Previous studies have

Table 1. Results and Summary of Findings from the Detailed Analysis of Field Samples Collected in 2019

diagnostic feature/method	output	significance			
Bulk Features of the Dichloromethane/Methanol Extract					
C, H, N, and S composition	83, 10, 0.7, and 3.6%	sulfur-rich petroleum			
simulated distillation	10, 30, 50, 70, and 90% at C20, C31, C43, C60, and C108, respectively	hydrocarbons span a wide carbon range and ~50% is non-GC-amenable			
SARA analysis by TLC-FID	9, 17, 49, and 25%	rich in resins and asphaltenes			
solubility in heptane	30%	contains significant amounts of polar material (i.e., resins and asphaltenes)			
¹³ C (‰)	-27‰	within the range expected for crude oils and comparable to values found in South American marginal oils ^d			
summary	mixture of petroleum HCs with elevated amounts of sulfur and polar, higher molecular-weight non-GC-amenable components				
Saturated HCs					
general features	HCs from C ₁₃ to C ₄₁ , including <i>n</i> -alkanes, on a smooth and continuous unresolved complex mixture	not a distillate cut over a discrete range (i.e., diesel, etc.)			
% of solvent extract is GC-amenable	25%	corroborates simulated distillation assessment of non-GC-amenable content			
total of individual <i>n</i> -alkanes and isoprenoids	10 700 mg/kg	no extensive biodegradation			
resolved/unresolved	5%	most GC-amenable material is not resolved			
<i>n</i> -C ₁₇ /pristane	1.8	no extensive biodegradation			
<i>n</i> -C ₁₈ /phytane	2.1	no extensive biodegradation			
odd/even preference (<i>n</i> -C ₁₄ to <i>n</i> -C ₄₀)	0.93	minimal or no input from plant wax <i>n</i> -alkanes			
fatty acid methyl acids	not detected	unlikely a biodiesel			
summary	mixture of petroleum HCs with elevated amounts of sulfur and polar, higher molecular-weight non-GC-amenable components; not extensively biodegraded				
	PAH^b	output	pyrogenic	petrogenic	determination^{b,c,d,e}
	phenanthrene/anthracene	7.8	<10	>15	pyrogenic
	C ₁ -phenanthrene/phenanthrene	33	<1	>5	petrogenic
	(C ₁ -phenanthrenes + C ₁ -anthracenes)/(phenanthrene + anthracene)	4	<1	>1.5	petrogenic
	fluoranthene/pyrene	0.15	>1.5	<0.5	petrogenic
	(C ₁ -fluoranthenes + pyrenes)/pyrene	3.27	~0.3	~4	petrogenic
	(C ₁ -fluoranthenes + C ₁ -pyrenes)/(fluoranthene + pyrene)	2.85	<0.5	>1	petrogenic
	benzo[<i>a</i>]anthracene/chrysene	0.37	>0.5	<0.5	petrogenic
	benzo[<i>e</i>]pyrene/benzo[<i>a</i>]pyrene	1.54	<1		not pyrogenic
	indeno[1,2,3- <i>c,d</i>]pyrene/benzo[<i>g,h,i</i>]perylene	0.28	>1	<0.25	indeterminate
	pyrene/benzo[<i>a</i>]pyrene	4.07	≪10	>10	indeterminate
	parent PAHs/alkylated PAHs	0.04	>0.5	<0.3	petrogenic
	anthracene/(anthracene + phenanthrene)	0.89	>0.5	<0.1	pyrogenic
	fluoranthene/(fluoranthene + pyrene)	0.13	>0.5	<0.1	indeterminate
	benzo(<i>a</i>)anthracene/(benzo[<i>a</i>]anthracene + chrysene)	0.27	>0.5	<0.1	indeterminate
	2-methylanthracene/∑ (C ₁ -phenanthrenes + C ₁ -anthracenes)	0.05	similar to modern heavy fuel oils (0.04 to 0.09) containing cracked materials ^c		
	(2-/3- + 1-methylbenzothiophene)/4-methylbenzothiophene	1.1	unlikely a virgin crude and includes thermally altered material		
	summary	PAH distribution consistent with petrogenic source; elevated five- to six-ring PAHs and diagnostic indicators support inputs from a thermally treated petroleum. Unlikely a virgin crude			
diagnostic feature/method	output	significance			
biomarkers					
oleanane/hopane	0.08	source rock early-to-late Cretaceous ^f .			
C ₂₇ /C ₂₉ sterane	1.02	marine or marginal marine (i.e., estuarine/deltaic) depositional environment and marine organic matter input ^{g,h}			
C ₂₃ tricyclic terpane/hopane ^c	~1	marine or marginal marine (i.e., estuarine/deltaic) depositional environment and marine organic matter input ^{g,h}			
C ₂₃ tricyclic terpane/C ₂₄ tetracyclic terpane ^e	8.96	marine or marginal marine (i.e., estuarine/deltaic) depositional environment and marine organic matter input ^{g,h}			
8,14-secohopane	detected	associated with in-reservoir biodegradation ⁱ			
25-norhopanes	detected	associated with in-reservoir biodegradation ^{j,k}			
Diginane	detected	associated with increased thermal maturity and some marginal South Atlantic oils ^{l,m}			
carotenoid biomarkers	detected	diagnostic for green and purple sulfur bacteria supports the low oxygen, sulfidic depositional environment, i.e., euxinia ⁿ			
summary	diagnostic molecules (biomarkers) are indicative of marginal South American crude oil; some indication of in-reservoir biodegradation counter to the presence of <i>n</i> -alkanes and suggests a mixture(s) of oils of different biodegradation levels, i.e., lightly and heavily biodegraded ^o .				

Table 1. continued

^aMello et al. (1988).⁷⁰ ^bStogiannidis and Laane (2015).¹⁰⁶ ^cUhler et al. (2016).⁴¹ ^dEmsbo-Mattingly and Litman (2016).⁴⁴ ^eWang and Fingas (1995).⁴⁶ ^fMoldowan et al. (1994).⁶³ ^gPeters et al. (2007).⁵¹ ^hEl Diasty and Moldowan (2012).⁵² ⁱOliveira et al. (2012).⁵⁶ ^jLópez et al. (2015).⁵³ ^kBennett et al. (2006).⁵⁷ ^lSchiefelbein et al. (2000).⁷² ^mYang et al. (2014).⁷¹ ⁿFrench et al. (2015).⁶⁵ ^oEscobar et al. (2020).³

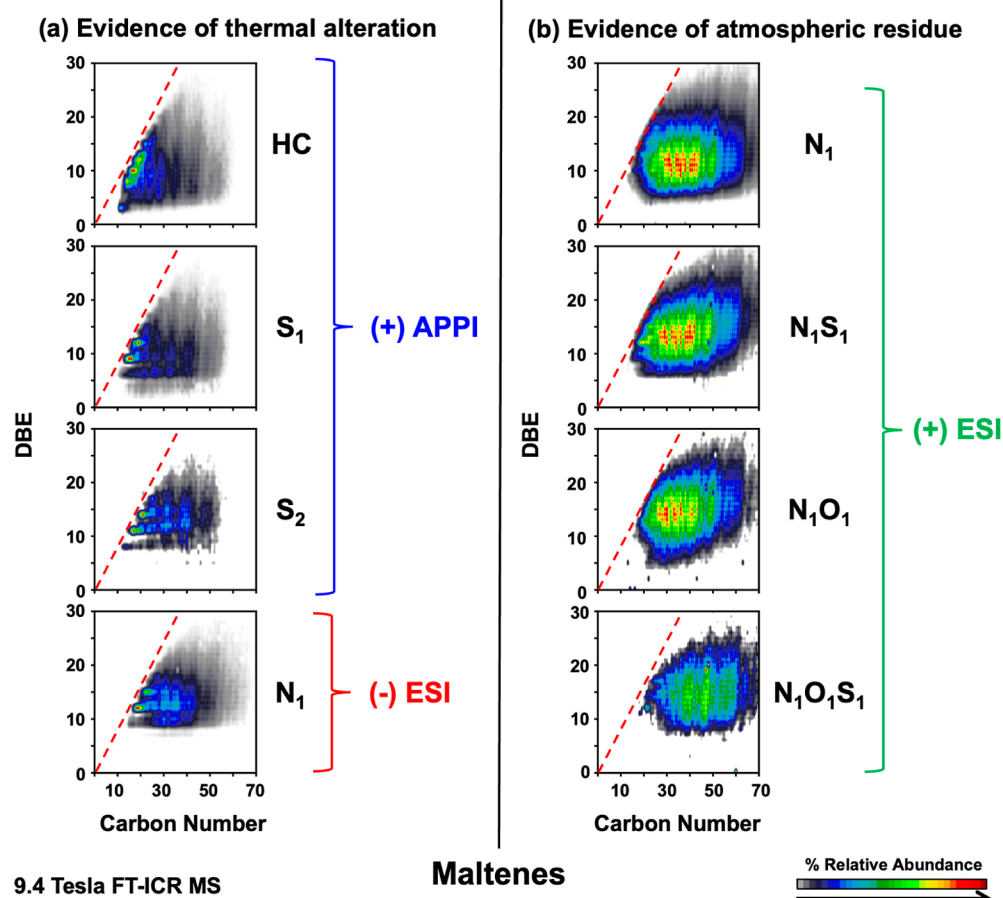


Figure 8. Color contour plots of DBE versus carbon number for (+) ESI, (+) APPI, and (-) ESI 9.4 T FT-ICR MS analysis of the maltene fraction. (A) Presence of species with increased DBE and lower alkylation, indicative of thermal alteration. (B) Compound classes with extended alkylated series ($\sim C_{20}$ – C_{70}). Although such extents of alkylation are typical for heavy crude oils,¹⁰⁷ the absence of species below C_{20} , rapid increase in relative abundance from C_{20} – C_{30} , combined with a gradual drop-off in the relative abundance at $C_{60+}/DBE > 10$, suggest the material is an atmospheric residue.

associated these biomarkers with extensive biodegradation and hence would contradict the limited biodegradation (*n*-alkanes present). One explanation would be that the mystery oil is a mixture of nondegraded and degraded oil. In summary, GC-based analyses of field samples from the Brazil mystery oil spill tell us that the spilled oil is not solely a crude oil but possibly a mixture (Table 1).

FT-ICR MS Analysis. To support and expand on GC-based analyses, field samples were analyzed by FT-ICR MS. Compared to GC, this high-resolution MS technique provides the molecular analysis of complex organic mixtures over a much wider boiling point range ($C_{10} < C_{120}$),⁷⁴ has a greater capacity to analyze polar and thermally labile compounds,⁷⁵ and can disentangle the components of multicomponent mixtures or blends.⁷⁶ Here, we sought to confirm or explore the possibility (or not) that the spilled oil contains higher boiling compounds indicative of (a) blending/mixing of crude oil with other petroleum products and (b) thermal alteration. Positive and negative (\pm) ESI and (+) APPI ionization methods were employed to provide complementary composi-

tional information.⁷⁵ ESI preferentially ionizes polar N-, S-, and O-containing species, whereas positive APPI is more suitable for ionizing HCs, condensed aromatics, and sulfur-bearing species.^{77,78}

The whole toluene/THF/methanol extracts of samples 1, 5, 6, and 12 were analyzed by (\pm) ESI and (+) APPI FT-ICR MS. The mass spectra were typical for crude oil and petroleum products based on the molecular mass distribution, elemental composition, and trends of heteroatom class, double-bond equivalents (DBE), and carbon number (DBE is the number of rings plus double bonds to carbon in a molecule).⁷⁹ Consistent with the GC-based results, Samples 1, 5, and 12 were similar and differed from Sample 6 (Figures 2 and S3). The whole extract of Sample 12 was separated into a maltene (heptane-soluble) and an asphaltene fraction (heptane-insoluble). Both fractions of Sample 12 were analyzed by (\pm) ESI and (+) APPI FT-ICR MS (Figures 8–10).

Maltenes. The heteroatom class graphs of the Sample 12 maltene fraction analyzed by (+) APPI would be classified as high-sulfur petroleum (elevated S_1 and S_2 class relative

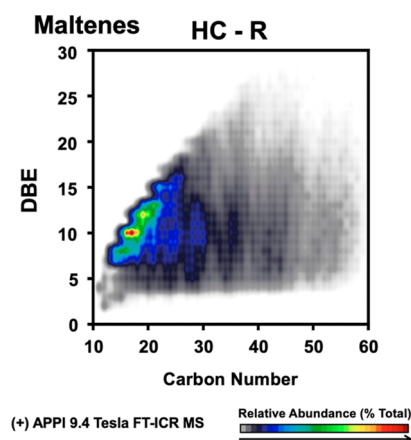


Figure 9. DBE versus carbon number plot for radical cations from the HC compound class reveals a diagonal distribution of abundant 2-, 3-, and 4-ring PAHs (in green, yellow, and red), indicative of near-bare or alkyl-deficient PAH species. Such abundant species are produced from the thermal alteration of higher boiling petroleum components.

abundances, Figure S10a), which agrees with the bulk elemental analysis of the whole extract (3.6% S). Similar trends of enriched sulfur-bearing species were observed for the (\pm) ESI class graphs (Figure S10b,c) with abundant N_1S_1 ((\pm) ESI), N_1S_2 ($(-)$ ESI), and O_xS_y ((\pm) ESI) species.

Analysis of the maltene fraction by (+) ESI FT-ICR MS revealed a carbon number distribution ($20 < C_{\#} < 70+$) and aromaticity range ($5 < DBE < 30$), typical of a heavy crude oil (Figure 8b).^{80,81} However, there is an absence of species below C_{20} and an abrupt increase in the relative abundance of species in the 20–30 carbon number range. Two possible explanations for the missing material less than C_{20} are removal at the refinery (distillation) or in the environment (evaporative weathering). Closer inspection of the results supports distillation. Evaporation generally leads to a gradual shift with the carbon number. The distinct transition at C_{20} is more typical of petroleum refining. In addition, there is a gradual drop in relative abundance (black to light gray) at high carbon numbers ($>C_{60}$) and DBE (>20), also typical of the residual stream of petroleum refining.⁸² Furthermore, the absence of species below C_{23} in the N_1 class (pyridinic nitrogen) indicates that the initial boiling point of the residuum is ~ 375 °C.⁸⁰ This temperature is similar to the final operating temperature (400

°C) for crude (or atmospheric) distillation units at petroleum refineries and consistent with the characteristics of an atmospheric distillation residuum.⁸²

Subsequent analysis of the maltene fraction of Sample 12 by ($-$) ESI and (+) APPI FT-ICR MS yielded much lower and narrower carbon number distributions ($10 < C_{\#} < 30$) that were shifted down in carbon number but upward in DBE toward the planar PAH limit line for the most abundant species (Figure 8a).⁸³ These dramatic compositional variations are evident in equally dramatic differences between the (+) ESI and (+) APPI molecular weight distributions in the broadband mass spectra (Figure S11). Here, the (+) ESI molecular weight distribution begins at ~ 200 Da with a pseudo-Gaussian distribution that peaks near 500 Da and ends at ~ 1100 Da. Conversely, the (+) APPI molecular weight distribution starts below 200 Da, peaks at ~ 225 Da, and decreases rapidly beyond 300 Da. Similar characteristics were noted for the ($-$) ESI data (Figure 8a). The high aromaticity (DBE), low carbon number, high relative abundance, and proximity of these species to the PAH limit line are consistent with a thermally altered material.⁸³ Furthermore, such a dramatic difference in the compositional space (carbon number range, DBE, and relative abundance) within a single maltene fraction as a function of different ionization methods is consistent with a blend that contains at least two components, an atmospheric residuum and a material that has experienced some form of thermal alteration (e.g., coking and visbreaking).^{82,84}

Thermal processing of vacuum residua produces abundant distillables (maltenes) containing one- to five-ring aromatics^{85,86} that are preferentially highlighted as radical molecular ions by APPI.⁷⁵ The maltene HC class (APPI, radical ions only) plot of carbon number versus DBE highlights the presence of abundant two- (DBE = 7), three- (DBE = 10), and four-ring (DBE = 13) PAHs with limited alkylation (0–5 methyl equivalents; Figure 9). The most abundant HC species detected in (+) APPI FT-ICR MS are the alkylated phenanthrenes/anthracenes (DBE 10), which is consistent with the GC-based results (Figure 3b), indicating that the field sample contains a material that has experienced thermal alteration.

Asphaltenes. Thermal processing also produces coke, abundant in highly dealkylated PAHs with five or more rings that are preferentially enriched in the asphaltene fraction. Thus, we chose to isolate the asphaltene fraction from Sample

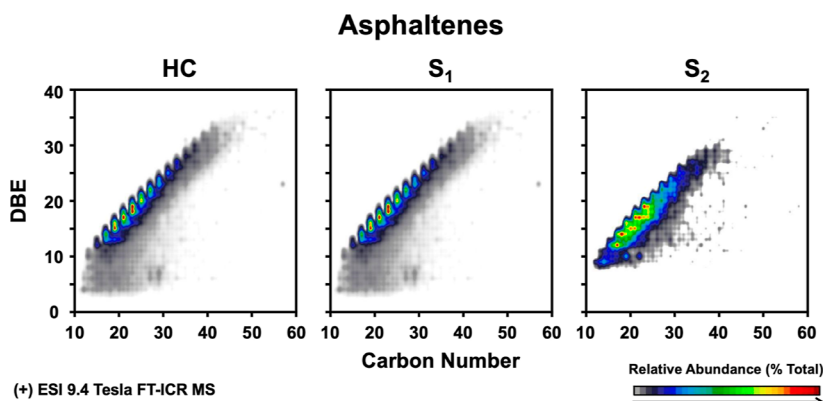


Figure 10. DBE versus carbon number plots for abundant compound classes (HC, S_1 , and S_2) for the asphaltene fraction illustrate the presence of abundant, aromatic-rich, and alkyl-deficient PAHs (4–14 ring) that suggest that they are the products of thermal alteration and undistilled prior to suspected blending.

12 to determine if such dealkylated PAH species are present, which would provide further evidence of thermal alteration. The (+) ESI FT-ICR MS analysis of the asphaltene fraction (HC, S₁, and S₂ classes shown in Figure 10) detected highly aromatic and alkyl-deficient PAHs (near bare PAHs), which confirms the suspected thermal alteration of at least one of the materials that comprise the sample extract. Although similar species have been observed in a few other asphaltene samples from South America,^{87,88} these data are unique because the relative abundance is defined to specific carbon numbers and DBE values that correspond to each successive aromatic ring addition to a growing PAH core (diagonal “dots” of high relative abundance along the PAH limit line). The wide expanse from 3 rings (DBE = 10, C_# = 14) to 14+ rings (DBE > 30, C_# > 40) establishes that the thermally altered component has not been distilled. Combined with the results from the analysis of the maltenes discussed above (Figures 8 and 9), some fraction of Sample 12 is the undistilled product of thermal alteration.

In summary, the unexpected compositional trends between the (+) ESI data and that of (−) ESI and (+) AAPI data of the maltene fraction indicate the Brazil mystery oil is a mixed product. The continuous, wide carbon number distributions for a broad range of DBE values observed by (+) ESI suggest the material is whole heavy crude. However, the lack of abundant species below C₂₀ and the anomalous, rapid increase in the relative abundance of species between C₂₀ and C₃₀ is indicative of an atmospheric residuum. Conversely, the (−) ESI and (+) AAPI data of the asphaltene fraction contain abundant one- to five-ring PAH species with low extents of alkylation that lie against the PAH limit line. The wide range of PAHs (3 to 14 rings) (+) ESI results are consistent with a highly aromatic, thermally altered oil that was not distilled prior to blending. Overall, field samples from the Brazil mystery oil have mass spectral features consistent with the blending of, at least, two different refined products, commonly done to provide an “on spec” product for marine fuel oils (e.g., bunkers).

Summary. Identifying the source and type of oil during a mystery spill, even with the most advanced techniques, is inherently uncertain.⁸⁹ Speculation should be avoided or minimized. Direct comparisons to possible sources using the known literature and library samples are limited because analytical data on many oils from around the world are not publicly available, and methods and instrumentation are not standardized. Any comparisons must also consider the effects of weathering, which removes some diagnostic markers, increases the number of probable sources, and reduces the analytical window for fingerprinting.⁸⁹ Our approach was to therefore employ a wide range of analytical results to comprehensively outline the chemical composition of the spilled oil, and, lacking suspect source oil(s) samples, eliminate the types of oils which, based on our analytical results and the literature, are unlikely to be the source.

The elevated bulk sulfur content (3.6%) eliminates a low-sulfur crude oil or low-sulfur fuel oil as a potential source. Given the abiotic loss of some fraction of the lighter ends (Figure 2), the original “spilled material” would have been below 3.5%, the maximum sulfur content for an intermediate fuel oil in 2019.⁹⁰ New regulations implemented in January 2020 lowered the allowable sulfur content to ≤ 0.5%.^{90,91} A combined amount of resins and asphaltenes (75%) excludes most distilled products and light crude oils.⁹² Environmental

weathering will presumably enrich the resins and asphaltenes, but given the moderate weathering in these samples, the elevated resin and asphaltene content is thought to be related to the source of the spilled oil. The bulk properties and HTSD are also consistent with the potential sources identified from the visual inspection of the GC-FID chromatograms, as discussed below.

Chromatographic and high-resolution MS analyses additionally eliminate some fresh and weathered petroleum products, such as synthetic motor oils and biodiesel blends (e.g., Peacock et al., 2010),⁹³ or even complex mixtures of synthetic chemicals such as toxaphene and PCBs. Moreover, the broad range of boiling points also excludes distillate sources with a “narrow” elution window, including products solely composed of gasoline, kerosene, diesel fuel, biodiesel, petroleum-based lubricating and hydraulic oils, low- and high-viscosity gas oils, vacuum oil, petroleum asphalt, and so forth.^{38,89,94,95} Both GC and FT-ICR MS indicate compounds/trends unlikely to be found in crude oil and produced at a refinery. Last, FT-ICR MS analyses reveal a component consistent with the residuum of atmospheric distillation.

With the above sources excluded and specific features the Brazil mystery oil was likely a fuel oil used for underway power of a vessel or transported for future use. These results alone cannot discount a shipwreck from WWII⁹⁶ (Figure 1) as it is possible that a refinery equipped with a delayed coker could have produced a product similar to the mystery oil. More than 500 shipwrecks from WWII are known to exist in the South Atlantic Ocean,⁹⁷ and it increasingly presents itself as a potential polluter of the oceans.^{13,96} In this sense, rubber bales from the SS *Rio Grande* shipwreck (Figure 1) arrived along the northeast of the Brazilian coast in 2018.⁹⁷ The release of this cargo was attributed to the natural corrosion of the shipwreck hull or unauthorized salvage of its metal cargo,⁹⁷ which may also have released the oil. However, more investigation is needed as the appearance of ancient raw material and the possibility of oil produced in the 1940s and 1950s emerge as strong evidence of the contribution of shipwrecks.

The results of this study show an overall similarity of oil residues collected in 2019 along the Brazilian coastline and help constrain the release location, source, and type of the mystery oil.

Oily residues collected in 2019 from northeast Brazil share the same source as those collected in 2019 at distances as far away as ~2400 km along the coastline (Figure 1).^{8,10,11} The significance of a sole source across this distance is threefold. First, samples from the aforementioned studies were collected north and south of the bifurcation, supporting the area of release to within the southern branch of sSEC or in the waters close to its bifurcation (Figure 1). Recently discovered natural HC seeps on the North São Paulo Plateau at ~20°S are an improbable source due to their location below the sSEC bifurcation and the lack of compositional differences between northern and southern samples (Figure 1).

Second, oiling over ~25 degrees of latitude provides a unique opportunity to monitor the short- and long-term fate of the remaining residues whether from evaporation, solubilization, microbial degradation, and/or photodegradation.⁹⁸ For example, the photochemical degradation rates on oil may be twice as fast at 0 than 30° latitude in winter months.⁹⁹ In addition, tracking the combined effects of weathering will be useful when disentangling the future chronic or acute releases of petroleum HCs via discrete, and ideally unique, molecular

markers such as ACLs, carotenoid-derived HCs or broadly across chromatographic and/or mass spectral space with GC \times GC^{15,100,101} and FT-ICR MS.²⁴

Last, the extent of coastal oiling relative to the estimated volume spilled was extreme compared to other spills (~3200 km). While the total volume of spilled oil remains unknown for the 2019 Brazil mystery oil spill, estimates range from 5 to 12.5 million liters.¹⁰² For comparison, approximately 632 million liters of oil flowed from the damaged Macondo well following the explosion of the *Deepwater Horizon* drilling rig, oiling ~1800 km of shoreline along the US Gulf states of Louisiana, Mississippi, Alabama, and Florida.¹⁰³ This finding may simply point to the effectiveness of ocean boundary currents to transport the spilled oil along the Brazilian coastline, or perhaps the amount of spilled oil was greater than the latest estimates.

Future Perspectives and Recommendations. It has been reported that cleanup of the spilled residues in sandy beaches has been partially successful.¹ However, the presence of oil on the Brazilian carbonate continental shelf, in mangroves, and on intertidal reefs is detected to this day.¹ Nevertheless, sustained monitoring is warranted in order to validate the effectiveness of restoration measures, monitor the fate and impacts of any remaining oil contamination, as well as to confirm no new oil pollution from chronic or acute releases is linked to the 2019 Brazil mystery oil spill.

In addition, refined estimates of the volume of oil spilled would be beneficial in eliminating possible sources. For example, the upper estimate of 12.5 million liters¹⁰² is close to the maximum capacity of fuel tanks of ocean-going cargo vessels and tankers (1.5 to 15 million liters¹⁰⁴) but considerably less than the maximum capacity of tankers that carry fuel oil (~110 million liters¹⁰⁵).

A continued and concerted effort will be required to compare the existing and future results of fingerprinting analyses with the existing oil and chemical databases, archival samples, and literature data. These efforts should focus on crude oils and petroleum products being sourced and transported in this region. Unique and specific markers, such as the ones reported in this study, analyzed with advanced instrumental tools, will be particularly valuable for robust source identification.

■ ASSOCIATED CONTENT

SI Supporting Information

The Supporting Information is available free of charge at <https://pubs.acs.org/doi/10.1021/acs.energyfuels.2c00656>.

Detailed analytical methods; sample locations; saturated HCs, PAHs, and biomarker content; map; sample photographs; GC-FID chromatograms; simulated distillation curve; extracted ion current GC-MS chromatograms; GC \times GC-FID chromatograms; difference chromatograms; and compound class designation and mass spectrum from FT-ICR MS (PDF)

GC \times GC-HRT mass spectra of biomarkers (PDF)

■ AUTHOR INFORMATION

Corresponding Author

Christopher M. Reddy – Department of Marine Chemistry and Geochemistry, Woods Hole Oceanographic Institution, Woods Hole, Massachusetts 02543, United States;

orcid.org/0000-0002-7814-2071; Phone: 858-514-6787; Email: creddy@whoi.edu

Authors

Robert K. Nelson – Department of Marine Chemistry and Geochemistry, Woods Hole Oceanographic Institution, Woods Hole, Massachusetts 02543, United States; orcid.org/0000-0003-0534-5801

Ulrich M. Hanke – Department of Marine Chemistry and Geochemistry, Woods Hole Oceanographic Institution, Woods Hole, Massachusetts 02543, United States

Xingqian Cui – Department of Earth, Atmospheric, and Planetary Sciences, Massachusetts Institute of Technology, Cambridge, Massachusetts 02142, United States

Roger E. Summons – Department of Earth, Atmospheric, and Planetary Sciences, Massachusetts Institute of Technology, Cambridge, Massachusetts 02142, United States

David L. Valentine – Department of Earth Science and Marine Science Institute, University of California, Santa Barbara, California 93106, United States

Ryan P. Rodgers – Ion Cyclotron Resonance Program, National High Magnetic Field Laboratory, Tallahassee, Florida 32310, United States; Department of Chemistry and Biochemistry, Florida State University, Tallahassee, Florida 32306, United States; orcid.org/0000-0003-1302-2850

Martha L. Chacón-Patiño – Ion Cyclotron Resonance Program, National High Magnetic Field Laboratory, Tallahassee, Florida 32310, United States; orcid.org/0000-0002-7273-5343

Sydney F. Niles – Ion Cyclotron Resonance Program, National High Magnetic Field Laboratory, Tallahassee, Florida 32310, United States; Department of Chemistry and Biochemistry, Florida State University, Tallahassee, Florida 32306, United States; orcid.org/0000-0002-3487-6612

Carlos E.P. Teixeira – Instituto de Ciências do Mar-LABOMAR, Federal University of Ceará, Fortaleza, CE 60440900, Brazil; Institut de Ciència i Tecnologia Ambientals (ICTA), Universitat Autònoma de Barcelona (UAB), Barcelona 08193, Spain

Luis E.A. Bezerra – Instituto de Ciências do Mar-LABOMAR, Federal University of Ceará, Fortaleza, CE 60440900, Brazil

Rivelino M. Cavalcante – Instituto de Ciências do Mar-LABOMAR, Federal University of Ceará, Fortaleza, CE 60440900, Brazil

Marcelo O. Soares – Instituto de Ciências do Mar-LABOMAR, Federal University of Ceará, Fortaleza, CE 60440900, Brazil; Leibniz Center for Tropical Marine Research (ZMT), Bremen 28359, Germany

André H.B. Oliveira – Department of Analytical Chemistry and Physical Chemistry, Federal University of Ceará, Fortaleza, CE 60440900, Brazil

Helen K. White – Department of Chemistry, Haverford College, Haverford, Pennsylvania 19041, United States

Robert F. Swarthout – A.R. Smith Department of Chemistry and Fermentation Sciences, Appalachian State University, Boone, North Carolina 28608, United States

Karin L. Lemkau – Department of Chemistry, Western Washington University, Bellingham, Washington 98225, United States

Jagoš R. Radović – Department of Geoscience, University of Calgary, T2N 1N4 Calgary, AB, Canada; orcid.org/0000-0002-6015-6416

Complete contact information is available at:

<https://pubs.acs.org/10.1021/acs.energyfuels.2c00656>

Author Contributions

C.M.R. and J.R.R. led and coordinated this study. M.O.S., C.E.P.T., L.E.A.B., A.H.B.O., and R.M.C. collected and sent the samples and contributed to the preparation of the article. R.K.N. performed GC×GC analyses, U.H. analyzed the samples by GC-FID and stable carbon isotope ratios. X.C. and R.E.S. performed GC-QQQ-MS analysis, and R.P.R., M.L.C., and S.F.N. contributed with FT-ICR MS results. C.M.R. and J.R.R. wrote major portions of the manuscript. K.L.L., R.F.S., and H.K.W. edited the final drafts. All authors contributed to the manuscript writing and revisions.

Notes

The authors declare no competing financial interest.

ACKNOWLEDGMENTS

Cassia Armstrong (WHOI) performed the SARA analysis. The authors have benefited from discussions and exchanges with Collin Ward (WHOI), Bryan James (WHOI), Jacqui Michel (Research Planning), Ed George (Bradford Soapworks), David Soud (I.R. Consilium), Scott Stout (Newfields), and Dan Villalanti (Triton Analytics). Edward Overton (LSU) and Martice Vasquez (California Department of Fish and Wildlife) provided analyses of several fuel oils. David Conlin (National Park Service) is acknowledged for sharing oil samples recently released from the USS *Arizona*. Zeyu Yang, Keval Shah, and Bruce Hollebone (Environment and Climate Change Canada) shared oil samples and unpublished results with the authors. Lorne Fell, Joe Binkley, Christina Kelly, and Anthony Toms (LECO) helped with the technical support of GC × GC instruments. R.M.C. is grateful for the PQ-2 grant (308216/2017-2-CNPq), INCT-AmbTropic phase II (CNPq Process 465634/2014-1) and project “Dispersants and adsorbents for remediation of coastal areas affected by crude oil spills (Coast of Ceará, Northeast Brazil) (440868/2020-3), both linked to MCTI Emergency Action to combat the oil spill (2020). C.E.P. Teixeira thanks FUNCAP/PRONEM PNE-0112-00007.01.00/16 and CAPES-PRINT for the financial support. M.O.S. thanks Conselho Nacional de Desenvolvimento Científico e Tecnológico (Research Productivity Fellowship 313518/2020–3), PELD Costa Semiárida do Brasil-CSB (no. 442337/2020-5), CAPES-PRINT, CAPES-Von Humboldt (AVH), and Fundação Cearense de Apoio ao Desenvolvimento Científico e Tecnológico (Chief Scientist Program) for their financial support. L.E.A.B. thanks Conselho Nacional de Desenvolvimento Científico e Tecnológico (Research Productivity Fellowship 310165/2020-2) and Fundação Cearense de Apoio ao Desenvolvimento Científico e Tecnológico (Chief Scientist Program) for their financial support. This project was also supported by NSF grant nos. OCE-1635562, OCE-1536346, OCE-1756254, OCE-1634478, OCE-1756242, OCE-1756947, and OCE-1756667. The FT-ICR MS work was supported by the National Science Foundation Division of Chemistry (through DMR-1644779), Florida State University, and the State of Florida.

REFERENCES

(1) Soares, M. O.; Teixeira, C. E. P.; Bezerra, L. E. A.; Rabelo, E. F.; Castro, I. B.; Cavalcante, R. M. The Most Extensive Oil Spill Registered in Tropical Oceans (Brazil): The Balance Sheet of a Disaster. *Environ. Sci. Pollut. Res.* **2022**, *29*, 19869–19877.

(2) Soares, M. O.; Teixeira, C. E. P.; Bezerra, L. E. A.; Rossi, S.; Tavares, T.; Cavalcante, R. M. Brazil Oil Spill Response: Time for Coordination. *Science* **2020**, *367*, 155.

(3) Escobar, M.; Márquez, G.; Guerrero, B.; Marín, P.; Boente, C.; Bernardo-Sánchez, A.; Romero, E.; Permanyer, A. Origin and Biodegradation of Crude Oils from the Northernmost Fields in the Bolívar Coastal Complex (Zulia State, Venezuela). *Energies* **2020**, *13*, 5615.

(4) Nasri Sissini, M.; Berchez, F.; Hall-Spencer, J.; Ghilardi-Lopes, N.; Carvalho, V. F.; Schubert, N.; Koerich, G.; Diaz-Pulido, G.; Silva, J.; Serrão, E.; Assis, J.; Santos, R.; Floeter, S. R.; Rörig, L.; Barufi, J. B.; Bernardino, A. F.; Francini-Filho, R.; Turra, A.; Hofmann, L. C.; Aguirre, J.; Le Gall, L.; Peña, V.; Nash, M. C.; Rossi, S.; Soares, M.; Pereira-Filho, G.; Tâmega, F.; Horta, P. A. Brazil Oil Spill Response: Protect Rhodolith Beds. *Science* **2020**, *367*, 156.

(5) Magalhães, K. M.; de SouzaBarros, K. V.; de Lima, M. C. S.; de AlmeidaRocha-Barreira, C.; Rosa Filho, J. S.; de Oliveira Soares, M. de O. Oil Spill + COVID-19: A Disastrous Year for Brazilian Seagrass Conservation. *Sci. Total Environ.* **2021**, *764*, 142872.

(6) Magris, R. A.; Giarrizzo, T. Mysterious Oil Spill in the Atlantic Ocean Threatens Marine Biodiversity and Local People in Brazil. *Mar. Pollut. Bull.* **2020**, *153*, 110961.

(7) de Oliveira Soares, M.; Teixeira, C. E. P.; Bezerra, L. E. A.; Paiva, S. V.; Tavares, T. C. L.; Garcia, T. M.; de Araújo, J. T.; Campos, C. C.; Ferreira, S. M. C.; Matthews-Cascon, H.; Frota, A.; Mont’Alverne, T. C. F.; Silva, S. T.; Rabelo, E. F.; Barroso, C. X.; de Freitas, J. E. P.; de Melo Júnior, M.; de SantanaCampelo, R. P.; de Santana, C. S.; de Macedo Carneiro, P. B.; Meirelles, A. J.; Santos, B. A.; de Oliveira, A. H. B.; Horta, P.; Cavalcante, R. M. Oil Spill in South Atlantic (Brazil): Environmental and Governmental Disaster. *Mar. Pol.* **2020**, *115*, 103879.

(8) de Oliveira, O. M. C.; de S. Queiroz, S. A. F.; Cerqueira, J. R.; Soares, S. A. R.; Garcia, K. S.; Filho, A. P.; de L. da S. Rosa, L. M.; Suzart, C. M.; de L. Pinheiro, L. L.; Moreira, Í. T. A. Environmental Disaster in the Northeast Coast of Brazil: Forensic Geochemistry in the Identification of the Source of the Oily Material. *Mar. Pollut. Bull.* **2020**, *160*, 111597.

(9) Lessa, G. C.; Teixeira, C. E. P.; Pereira, J.; Santos, F. M. The 2019 Brazilian Oil Spill: Insights on the Physics behind the Drift. *J. Mar. Syst.* **2021**, *222*, 103586.

(10) Lourenço, R. A.; Combi, T.; Alexandre, M. da R.; Sasaki, S. T.; Zanardi-Lamardo, E.; Yogui, G. T. Mysterious oil spill along Brazil’s northeast and southeast seaboard (2019-2020): Trying to find answers and filling data gaps. *Mar. Pollut. Bull.* **2020**, *156*, 111219.

(11) Carregosa, J. C.; Santos, I. R.; de Sá, M. S.; Santos, J. M.; Wisniewski, A., Jr. Multiple Reaction Monitoring Tool Applied in the Geochemical Investigation of a Mysterious Oil Spill in Northeast Brazil. *An Acad. Bras Ciências* **2021**, *93*, No. e20210171.

(12) Zacharias, D. C.; Gama, C. M.; Harari, J.; da Rocha, R. P.; Fornaro, A. Mysterious oil spill on the Brazilian coast - Part 2: A probabilistic approach to fill gaps of uncertainties. *Mar. Pollut. Bull.* **2021**, *173*, 113085.

(13) Landquist, H.; Hassellöv, I.-M.; Rosén, L.; Lindgren, J. F.; Dahllöf, I. Evaluating the Needs of Risk Assessment Methods of Potentially Polluting Shipwrecks. *J. Environ. Manage.* **2013**, *119*, 85–92.

(14) Reuters in Brasília. Brazil blames devastating oil spill on Greek-flagged tanker. The Guardian. <https://www.theguardian.com/world/2019/nov/01/brazil-blames-oil-spill-greek-flagged-tanker-venezuelan-crude> (accessed June 16, 2022).

(15) Lemkau, K. L.; Peacock, E. E.; Nelson, R. K.; Ventura, G. T.; Kovacs, J. L.; Reddy, C. M. The M/V Cosco Busan Spill: Source Identification and Short-Term Fate. *Mar. Pollut. Bull.* **2010**, *60*, 2123–2129.

(16) Reddy, C. M.; Quinn, J. G. The North Cape Oil Spill: Hydrocarbons in Rhode Island Coastal Waters and Point Judith Pond. *Mar. Environ. Res.* **2001**, *52*, 445–461.

(17) Reddy, C. M.; Quinn, J. G. GC-MS Analysis of Total Petroleum Hydrocarbons and Polycyclic Aromatic Hydrocarbons in Seawater

Samples after the North Cape Oil Spill. *Mar. Pollut. Bull.* **1999**, *38*, 126–135.

(18) Maltezos, R.; Teixeira, M. Brazil adds four other tankers as suspects for oil spill. Reuters. <https://www.reuters.com/article/us-brazil-oil-spill-idUSKBN1XH009> (accessed June 12, 2022).

(19) Jansen, R.; dePaulo, S. O. E. Universidade afirma ter identificado navio que derramou óleo no litoral. Estadão. <https://sustentabilidade.estadao.com.br/noticias/geral,universidade-afirma-ter-identificado-navio-que-derramou-oleo-no-litoral,70003092982> (accessed June 12, 2022).

(20) Zanini, F. PF calcula dano mínimo de R\$ 188 milhões por vazamento de óleo e indicia gregos. Folha de São Paulo. <https://www1.folha.uol.com.br/colunas/painel/2021/12/pf-calcula-dano-minimo-de-r-188-milhoes-por-vazamento-de-oleo-e-indicia-gregos.shtml> (accessed June 12, 2022).

(21) Peters, K. E.; Scheuerman, G. L.; Lee, C. Y.; Moldowan, J. M.; Reynolds, R. N.; Pena, M. M. Effects of Refinery Processes on Biological Markers. *Energy Fuels* **1992**, *6*, 560–577.

(22) Gbadamosi, A. O.; Junin, R.; Manan, M. A.; Agi, A.; Yusuff, A. S. An Overview of Chemical Enhanced Oil Recovery: Recent Advances and Prospects. *Int. Nano Lett.* **2019**, *9*, 171–202.

(23) Scarlett, A. G.; Nelson, R. K.; Gagnon, M. M.; Holman, A. I.; Reddy, C. M.; Sutton, P. A.; Grice, K. MV Wakashio grounding incident in Mauritius 2020: The world's first major spillage of Very Low Sulfur Fuel Oil. *Mar. Pollut. Bull.* **2021**, *171*, 112917.

(24) Lemkau, K. L.; McKenna, A. M.; Podgorski, D. C.; Rodgers, R. P.; Reddy, C. M. Molecular Evidence of Heavy-Oil Weathering Following the M/V Cosco Busan Spill: Insights from Fourier Transform Ion Cyclotron Resonance Mass Spectrometry. *Environ. Sci. Technol.* **2014**, *48*, 3760–3767.

(25) Ruddy, B. M.; Huettel, M.; Kostka, J. E.; Lobodin, V. v.; Bythell, B. J.; McKenna, A. M.; Aeppli, C.; Reddy, C. M.; Nelson, R. K.; Marshall, A. G.; Rodgers, R. P. Targeted Petroleomics: Analytical Investigation of Macondo Well Oil Oxidation Products from Pensacola Beach. *Energy Fuels* **2014**, *28*, 4043–4050.

(26) Wise, S. A.; Rodgers, R. P.; Reddy, C. M.; Nelson, R. K.; Kujawinski, E. B.; Wade, T. L.; Campiglia, A. D.; Liu, Z. Advances in Chemical Analysis of Oil Spills Since the Deepwater Horizon Disaster. *Crit. Rev. Anal. Chem.* **2022**, 1–60.

(27) Chen, H.; Nelson, R. K.; Swarthout, R. F.; Shigenaka, G.; de Oliveira, A. H. B.; Reddy, C. M.; McKenna, A. M. Detailed Compositional Characterization of the 2014 Bangladesh Furnace Oil Released into the World's Largest Mangrove Forest. *Energy Fuels* **2018**, *32*, 3232–3242.

(28) Koolen, H. H. F.; Swarthout, R. F.; Nelson, R. K.; Chen, H.; Krajewski, L. C.; Aeppli, C.; McKenna, A. M.; Rodgers, R. P.; Reddy, C. M. Unprecedented Insights into the Chemical Complexity of Coal Tar from Comprehensive Two-Dimensional Gas Chromatography Mass Spectrometry and Direct Infusion Fourier Transform Ion Cyclotron Resonance Mass Spectrometry. *Energy Fuels* **2015**, *29*, 641–648.

(29) Eiserbeck, C.; Nelson, R. K.; Reddy, C. M.; Grice, K. *Advances in Comprehensive Two-Dimensional Gas Chromatography (GC × GC)*; Royal Society of Chemistry: London, 2014; Vol. 4.

(30) Aeppli, C.; Carmichael, C. A.; Nelson, R. K.; Lemkau, K. L.; Graham, W. M.; Redmond, M. C.; Valentine, D. L.; Reddy, C. M. Oil Weathering after the Deepwater Horizon Disaster Led to the Formation of Oxygenated Residues. *Environ. Sci. Technol.* **2012**, *46*, 8799–8807.

(31) Nelson, R. K.; Gosselin, K. M.; Hollander, D. J.; Murawski, S. A.; Gracia, A.; Reddy, C. M.; Radović, J. R. Exploring the Complexity of Two Iconic Crude Oil Spills in the Gulf of Mexico (Ixtoc I and Deepwater Horizon) Using Comprehensive Two-Dimensional Gas Chromatography (GC × GC). *Energy Fuels* **2019**, *33*, 3925–3933.

(32) Stout, S. A. Oil Spill Fingerprinting Method for Oily Matrices Used in the Deepwater Horizon NRDA. *Environ. Forensics* **2016**, *17*, 218–243.

(33) Roussel, A.; Cui, X.; Summons, R. E. Biomarker stratigraphy in the Athel Trough of the South Oman Salt Basin at the Ediacaran-Cambrian Boundary. *Geobiology* **2020**, *18*, 663–681.

(34) Kivenson, V.; Lemkau, K. L.; Pizarro, O.; Yoerger, D. R.; Kaiser, C.; Nelson, R. K.; Carmichael, C.; Paul, B. G.; Reddy, C. M.; Valentine, D. L. Ocean Dumping of Containerized DDT Waste Was a Sloppy Process. *Environ. Sci. Technol.* **2019**, *53*, 2971–2980.

(35) Kaiser, N. K.; Quinn, J. P.; Blakney, G. T.; Hendrickson, C. L.; Marshall, A. G. A Novel 9.4 Tesla FTICR Mass Spectrometer with Improved Sensitivity, Mass Resolution, and Mass Range. *J. Am. Soc. Mass Spectrom.* **2011**, *22*, 1343–1351.

(36) Nelson, R. K.; Aeppli, C.; Arey, J. S.; Chen, H.; de Oliveira, A. H. B.; Eiserbeck, C.; Frysinger, G. S.; Gaines, R. B.; Grice, K.; Gros, J.; Hall, G. J.; Koolen, H. H. F.; Lemkau, K. L.; McKenna, A. M.; Reddy, C. M.; Rodgers, R. P.; Swarthout, R. F.; Valentine, D. L.; White, H. K. Applications of comprehensive two-dimensional gas chromatography (GC × GC) in studying the source, transport, and fate of petroleum hydrocarbons in the environment. In *Standard Handbook Oil Spill Environmental Forensics*; Elsevier, 2016, pp 399–448. DOI: 10.1016/B978-0-12-803832-1.00008-8.

(37) Lemkau, K. L.; Reddy, C. M.; Carmichael, C. A.; Aeppli, C.; Swarthout, R. F.; White, H. K. Hurricane Isaac Brings More than Oil Ashore: Characteristics of Beach Deposits Following the Deepwater Horizon Spill. *PLoS One* **2019**, *14*, No. e0213464.

(38) Wang, Z.; Yang, C.; Yang, Z.; Brown, C. E.; Hollebone, B. P.; Stout, S. A. Petroleum Biomarker Fingerprinting for Oil Spill Characterization and Source Identification. In *Standard Handbook Oil Spill Environmental Forensics*; Elsevier, 2016, pp 131–254. DOI: 10.1016/B978-0-12-803832-1.00004-0.

(39) Overton, E.; Wade, T.; Radovic, J.; Meyer, B.; Miles, M. S.; Larter, S. Chemical Composition of Macondo and Other Crude Oils and Compositional Alterations During Oil Spills. *Oceanography* **2016**, *29*, 50–63.

(40) White, H. K.; Hsing, P.-Y.; Cho, W.; Shank, T. M.; Cordes, E. E.; Quattrini, A. M.; Nelson, R. K.; Camilli, R.; Demopoulos, A. W. J.; German, C. R.; Brooks, J. M.; Roberts, H. H.; Shedd, W.; Reddy, C. M.; Fisher, C. R. Impact of the Deepwater Horizon Oil Spill on a Deep-Water Coral Community in the Gulf of Mexico. *Proc. Natl. Acad. Sci. U.S.A.* **2012**, *109*, 20303–20308.

(41) Uhler, A. D.; Stout, S. A.; Douglas, G. S.; Healey, E. M.; Emsbo-Mattingly, S. D. Chemical Character of Marine Heavy Fuel Oils and Lubricants. In *Standard Handbook Oil Spill Environmental Forensics*; Elsevier, 2016, pp 641–683. DOI: 10.1016/B978-0-12-803832-1.00013-1.

(42) Sun, P.; Bao, M.; Li, F.; Cao, L.; Wang, X.; Zhou, Q.; Li, G.; Tang, H. Sensitivity and Identification Indexes for Fuel Oils and Crude Oils Based on the Hydrocarbon Components and Diagnostic Ratios Using Principal Component Analysis (PCA) Biplots. *Energy Fuels* **2015**, *29*, 3032–3040.

(43) Dahlman, G. Characteristic Features of Different Oil Types in Oil Spill Identification. *Berichte Bundesamtes Seeschifffahrt Hydrographie* **2003**, *31*, 1–48.

(44) Emsbo-Mattingly, S. D.; Litman, E. Polycyclic Aromatic Hydrocarbon Homolog and Isomer Fingerprinting. In *Standard Handbook Oil Spill Environmental Forensics*; Elsevier, 2016, pp 255–312. DOI: 10.1016/B978-0-12-803832-1.00005-2.

(45) Yang, Z.; Shah, K.; Laforest, S.; Hollebone, B. P.; Lambert, P.; Brown, C. E.; Yang, C.; Goldthorp, M. A Study of the 46-Year-Old Arrow Oil Spill: Persistence of Oil Residues and Variability in Oil Contamination along Chedabucto Bay, Nova Scotia, Canada. *J. Clean. Prod.* **2018**, *198*, 1459–1473.

(46) Wang, Z.; Fingas, M. Differentiation of the Source of Spilled Oil and Monitoring of the Oil Weathering Process Using Gas Chromatography-Mass Spectrometry. *J. Chromatogr., A* **1995**, *712*, 321–343.

(47) López, L. Study of the Biodegradation Levels of Oils from the Orinoco Oil Belt (Junin Area) Using Different Biodegradation Scales. *Org. Geochem.* **2014**, *66*, 60–69.

- (48) Ten Haven, H. L.; Rullkötter, J.; De Leeuw, J. W.; Damsté, J. S. Pristane/Phytane Ratio as Environmental Indicator. *Nature* **1988**, *333*, 604.
- (49) Sarmiento, L. F.; Rangel, A. Petroleum Systems of the Upper Magdalena Valley, Colombia. *Mar. Petrol. Geol.* **2004**, *21*, 373–391.
- (50) Hughes, W. B.; Holba, A. G.; Dzou, L. I. P. The Ratios of Dibenzothiophene to Phenanthrene and Pristane to Phytane as Indicators of Depositional Environment and Lithology of Petroleum Source Rocks. *Geochim. Cosmochim. Acta* **1995**, *59*, 3581–3598.
- (51) Peters, K. E.; Walters, C. C.; Moldowan, J. M. *The Biomarker Guide Volume 2 Biomarkers and Isotopes in Petroleum Systems and Earth History*, 2nd ed.; Cambridge University Press, 2007.
- (52) El Diasty, W. Sh.; Moldowan, J. M. Application of biological markers in the recognition of the geochemical characteristics of some crude oils from Abu Gharadig Basin, north Western Desert - Egypt. *Mar. Petrol. Geol.* **2012**, *35*, 28–40.
- (53) López, L.; Lo Mónaco, S.; Volkman, J. K. Evidence for Mixed and Biodegraded Crude Oils in the Socororo Field, Eastern Venezuela Basin. *Org. Geochem.* **2015**, *82*, 12–21.
- (54) Grantham, P. J.; Wakefield, L. L. Variations in the Sterane Carbon Number Distributions of Marine Source Rock Derived Crude Oils through Geological Time. *Org. Geochem.* **1988**, *12*, 61–73.
- (55) Knoll, A. H.; Summons, R. E.; Waldbauer, J. R.; Zumberge, J. E. The Geological Succession of Primary Producers in the Oceans. In *Evolution of Primary Producers in the Sea*; Elsevier, 2007, pp 133–163. DOI: 10.1016/B978-012370518-1/50009-6.
- (56) Oliveira, C. R.; Ferreira, A. A.; Oliveira, C. J. F.; Azevedo, D. A.; Santos Neto, E. v.; Aquino Neto, F. R. Biomarkers in Crude Oil Revealed by Comprehensive Two-Dimensional Gas Chromatography Time-of-Flight Mass Spectrometry: Depositional Paleoenvironment Proxies. *Org. Geochem.* **2012**, *46*, 154–164.
- (57) Bennett, B.; Fustic, M.; Farrimond, P.; Huang, H.; Larter, S. R. 25-Norhopanes: Formation during Biodegradation of Petroleum in the Subsurface. *Org. Geochem.* **2006**, *37*, 787–797.
- (58) López, L.; Lo Mónaco, S. Vanadium, Nickel and Sulfur in Crude Oils and Source Rocks and Their Relationship with Biomarkers: Implications for the Origin of Crude Oils in Venezuelan Basins. *Org. Geochem.* **2017**, *104*, 53–68.
- (59) Ventura, G. T.; Kenig, F.; Reddy, C. M.; Schieber, J.; Fryinger, G. S.; Nelson, R. K.; Dinel, E.; Gaines, R. B.; Schaeffer, P. Molecular Evidence of Late Archean Archaea and the Presence of a Subsurface Hydrothermal Biosphere. *Proc. Natl. Acad. Sci. U.S.A.* **2007**, *104*, 14260–14265.
- (60) De Leeuw, J. W.; Frewin, N. L.; Van Bergen, P. F.; Sinninghe Damsté, J. S.; Collinson, M. E. Organic Carbon as a Palaeoenvironmental Indicator in the Marine Realm. *Geological Society* **1995**, *83*, 43–71.
- (61) Wingert, W. S.; Pomerantz, M. Structure and Significance of Some Twenty-One and Twenty-Two Carbon Petroleum Steranes. *Geochim. Cosmochim. Acta* **1986**, *50*, 2763–2769.
- (62) Araújo, B. Q.; Azevedo, D. de A. Uncommon Steranes in Brazilian Marginal Crude Oils: Dinoflagellate Molecular Fossils in the Sergipe-Alagoas Basin, Brazil. *Org. Geochem.* **2016**, *99*, 38–52.
- (63) Moldowan, J. M.; Dahl, J.; Huizinga, B. J.; Fago, F. J.; Hickey, L. J.; Peakman, T. M.; Taylor, D. W. The Molecular Fossil Record of Oleanane and Its Relation to Angiosperms. *Science* **1994**, *265*, 768–771.
- (64) Holba, A. G.; Dzou, L. I. P.; Masterson, W. D.; Hughes, W. B.; Huizinga, B. J.; Singletary, M. S.; Moldowan, J. M.; Mello, M. R.; Tegelaar, E. Application of 24-Norcholestanes for Constraining Source Age of Petroleum. *Org. Geochem.* **1998**, *29*, 1269–1283.
- (65) French, K. L.; Rocher, D.; Zumberge, J. E.; Summons, R. E. Assessing the distribution of sedimentary C₄₀carotenoids through time. *Geobiology* **2015**, *13*, 139–151.
- (66) French, K. L.; Birdwell, J. E.; Vanden Berg, M. D. Biomarker Similarities between the Saline Lacustrine Eocene Green River and the Paleoproterozoic Barney Creek Formations. *Geochim. Cosmochim. Acta* **2020**, *274*, 228–245.
- (67) Summons, R. E.; Powell, T. G. Identification of Aryl Isoprenoids in Source Rocks and Crude Oils: Biological Markers for the Green Sulphur Bacteria. *Geochim. Cosmochim. Acta* **1987**, *51*, 557–566.
- (68) Summons, R. E.; Powell, T. G. Chlorobiaceae in Palaeozoic Seas Revealed by Biological Markers, Isotopes and Geology. *Nature* **1986**, *319*, 763–765.
- (69) Cui, X.; Liu, X.-L.; Shen, G.; Ma, J.; Husain, F.; Rocher, D.; Zumberge, J. E.; Bryant, D. A.; Summons, R. E. Niche expansion for phototrophic sulfur bacteria at the Proterozoic-Phanerozoic transition. *Proc. Natl. Acad. Sci. U.S.A.* **2020**, *117*, 17599–17606.
- (70) Mello, M. R.; Gaglianone, P. C.; Brassell, S. C.; Maxwell, J. R. Geochemical and Biological Marker Assessment of Depositional Environments Using Brazilian Offshore Oils. *Mar. Petrol. Geol.* **1988**, *5*, 205–223.
- (71) Yang, R.; Wang, Y.; Cao, J. Cretaceous Source Rocks and Associated Oil and Gas Resources in the World and China: A Review. *Petrol. Sci.* **2014**, *11*, 331–345.
- (72) Geochemical Comparison of Crude Oil Along South Atlantic Margins. In *Petroleum Systems of South Atlantic Margins*; American Association of Petroleum Geologists, 2000; pp 15–26.
- (73) Samuel, O. J.; Cornford, C.; Jones, M.; Adekeye, O. A.; Akande, S. O. Improved Understanding of the Petroleum Systems of the Niger Delta Basin, Nigeria. *Org. Geochem.* **2009**, *40*, 461–483.
- (74) McKenna, A. M.; Nelson, R. K.; Reddy, C. M.; Savory, J. J.; Kaiser, N. K.; Fitzsimmons, J. E.; Marshall, A. G.; Rodgers, R. P. Expansion of the Analytical Window for Oil Spill Characterization by Ultrahigh Resolution Mass Spectrometry: Beyond Gas Chromatography. *Environ. Sci. Technol.* **2013**, *47*, 7530–7539.
- (75) Purcell, J. M.; Rodgers, R. P.; Hendrickson, C. L.; Marshall, A. G. Speciation of Nitrogen Containing Aromatics by Atmospheric Pressure Photoionization or Electrospray Ionization Fourier Transform Ion Cyclotron Resonance Mass Spectrometry. *J. Am. Soc. Mass Spectrom.* **2007**, *18*, 1265–1273.
- (76) Witt, M.; Timm, W. Determination of Simulated Crude Oil Mixtures from the North Sea Using Atmospheric Pressure Photoionization Coupled to Fourier Transform Ion Cyclotron Resonance Mass Spectrometry. *Energy Fuels* **2016**, *30*, 3707–3713.
- (77) Purcell, J. M.; Hendrickson, C. L.; Rodgers, R. P.; Marshall, A. G. Atmospheric Pressure Photoionization Proton Transfer for Complex Organic Mixtures Investigated by Fourier Transform Ion Cyclotron Resonance Mass Spectrometry. *J. Am. Soc. Mass Spectrom.* **2007**, *18*, 1682–1689.
- (78) Gaspar, A.; Zeller, E.; Lababidi, S.; Reece, J.; Schrader, W. Impact of Different Ionization Methods on the Molecular Assignments of Asphaltenes by FT-ICR Mass Spectrometry. *Anal. Chem.* **2012**, *84*, 5257–5267.
- (79) Marshall, A. G.; Rodgers, R. P. Petroleumomics: Chemistry of the underworld. *Proc. Natl. Acad. Sci. U.S.A.* **2008**, *105*, 18090–18095.
- (80) Smith, D. F.; Rahimi, P.; Teclemariam, A.; Rodgers, R. P.; Marshall, A. G. Characterization of Athabasca Bitumen Heavy Vacuum Gas Oil Distillation Cuts by Negative/Positive Electrospray Ionization and Automated Liquid Injection Field Desorption Ionization Fourier Transform Ion Cyclotron Resonance Mass Spectrometry. *Energy Fuels* **2008**, *22*, 3118–3125.
- (81) McKenna, A. M.; Blakney, G. T.; Xian, F.; Glaser, P. B.; Rodgers, R. P.; Marshall, A. G. Heavy Petroleum Composition. 2. Progression of the Boduszynski Model to the Limit of Distillation by Ultrahigh-Resolution FT-ICR Mass Spectrometry. *Energy Fuels* **2010**, *24*, 2939–2946.
- (82) Parkash, S. *Refining Processes Handbook*, 1st ed.; Elsevier, 2003.
- (83) Hsu, C. S.; Lobodin, V. v.; Rodgers, R. P.; McKenna, A. M.; Marshall, A. G. Compositional Boundaries for Fossil Hydrocarbons. *Energy Fuels* **2011**, *25*, 2174–2178.
- (84) Purcell, J. M.; Merdignac, I.; Rodgers, R. P.; Marshall, A. G.; Gauthier, T.; Guibard, I. Stepwise Structural Characterization of Asphaltenes during Deep Hydroconversion Processes Determined by Atmospheric Pressure Photoionization (APPI) Fourier Transform Ion

Cyclotron Resonance (FT-ICR) Mass Spectrometry. *Energy Fuels* **2010**, *24*, 2257–2265.

(85) Strausz, O. P.; Mojelsky, T. W.; Faraji, F.; Lown, E. M.; Peng, P. Additional Structural Details on Athabasca Asphaltene and Their Ramifications. *Energy Fuels* **1999**, *13*, 207–227.

(86) Rueda-Velázquez, R. I.; Freund, H.; Qian, K.; Olmstead, W. N.; Gray, M. R. Characterization of Asphaltene Building Blocks by Cracking under Favorable Hydrogenation Conditions. *Energy Fuels* **2013**, *27*, 1817–1829.

(87) Chacón-Patiño, M. L.; Rowland, S. M.; Rodgers, R. P. Advances in Asphaltene Petroleomics. Part 1: Asphaltenes Are Composed of Abundant Island and Archipelago Structural Motifs. *Energy Fuels* **2017**, *31*, 13509–13518.

(88) Chacón-Patiño, M. L.; Rowland, S. M.; Rodgers, R. P. Advances in Asphaltene Petroleomics. Part 2: Selective Separation Method That Reveals Fractions Enriched in Island and Archipelago Structural Motifs by Mass Spectrometry. *Energy Fuels* **2018**, *32*, 314–328.

(89) Stout, S. A.; Wang, Z. Chemical Fingerprinting Methods and Factors Affecting Petroleum Fingerprints in the Environment. In *Standard Handbook Oil Spill Environmental Forensics*; Elsevier, 2016, pp 61–129. DOI: 10.1016/B978-0-12-803832-1.00003-9.

(90) International Maritime Organization. IMO 2020 – cutting sulphur oxide emissions. <https://www.imo.org/en/MediaCentre/HotTopics/Pages/Sulphur-2020.aspx> (accessed June 13 2022).

(91) Nelson, R. K.; Scarlett, A. G.; Gagnon, M. M.; Holman, A. I.; Reddy, C. M.; Sutton, P. A.; Grice, K. Characterizations and Comparison of Low Sulfur Fuel Oils Compliant with 2020 Global Sulfur Cap Regulation for International Shipping. *Mar. Pollut. Bull.* **2022**, *180*, 113791.

(92) Radović, J. R.; Domínguez, C.; Laffont, K.; Díez, S.; Readman, J. W.; Albaigés, J.; Bayona, J. M. Compositional Properties Characterizing Commonly Transported Oils and Controlling Their Fate in the Marine Environment. *Journal of Environmental Monitoring* **2012**, *14*, 3220.

(93) Peacock, E. E.; Arey, J. S.; DeMello, J. A.; McNichol, A. P.; Nelson, R. K.; Reddy, C. M. Molecular and Isotopic Analysis of Motor Oil from a Biodiesel-Driven Vehicle. *Energy Fuels* **2010**, *24*, 1037–1042.

(94) Kienhuis, P. G. M.; Hansen, A. B.; Faksness, L.-G.; Stout, S. A.; Dahlmann, G. CEN Methodology for Oil Spill Identification. In *Standard Handbook Oil Spill Environmental Forensics*; Elsevier, 2016, pp 685–728.

(95) ASTM International. ASTM D3328-06. *Standard Test Methods for Comparison of Waterborne Petroleum Oils by Gas Chromatography*. 2020. DOI: 10.1520/D3328-06R20

(96) Monfils, R. The global risk of marine pollution from WWII shipwrecks: examples from the seven seas. *Int. Oil Spill Conf. Proc.* **2005**, *2005*, 1049–1054.

(97) Teixeira, C. E. P.; Cavalcante, R. M.; Soares, M. O.; Ribeiro, F. B.; Bezerra, L. E. A. Marine Debris from the Past - Contamination of the Brazilian Shore by a WWII Wreck. *Mar. Environ. Res.* **2021**, *169*, 105345.

(98) Tarr, M.; Zito, P.; Overton, E.; Olson, G.; Adkikari, P.; Reddy, C. Weathering of Oil Spilled in the Marine Environment. *Oceanography* **2016**, *29*, 126–135.

(99) Freeman, D. H.; Ward, C. P. Sunlight-Driven Dissolution Is a Major Fate of Oil at Sea. *Sci. Adv.* **2022**, *8*, No. eabl7605.

(100) Arey, J. S.; Nelson, R. K.; Reddy, C. M. Disentangling Oil Weathering Using GC×GC. 1. Chromatogram Analysis. *Environ. Sci. Technol.* **2007**, *41*, 5738–5746.

(101) Arey, J. S.; Nelson, R. K.; Plata, D. L.; Reddy, C. M. Disentangling Oil Weathering Using GC×GC. 2. Mass Transfer Calculations. *Environ. Sci. Technol.* **2007**, *41*, 5747–5755.

(102) Zacharias, D. C.; Gama, C. M.; Fornaro, A. Mysterious Oil Spill on Brazilian Coast: Analysis and Estimates. *Mar. Pollut. Bull.* **2021**, *165*, 112125.

(103) Michel, J.; Owens, E. H.; Zengel, S.; Graham, A.; Nixon, Z.; Allard, T.; Holton, W.; Reimer, P. D.; Lamarche, A.; White, M.; Rutherford, N.; Childs, C.; Mauseth, G.; Challenger, G.; Taylor, E.

Extent and Degree of Shoreline Oiling: Deepwater Horizon Oil Spill, Gulf of Mexico, USA. *PLoS One* **2013**, *8*, No. e65087.

(104) National Oceanic and Atmospheric Administration (NOAA) Office of Response and Restoration. How Much Oil Is on That Ship?. <https://response.restoration.noaa.gov/about/media/how-much-oil-ship.html> (accessed June 13, 2022).

(105) U.S. Energy Information Administration. Oil tanker sizes range from general purpose to ultra-large crude carriers on AFRA scale. <https://www.eia.gov/todayinenergy/detail.php?id=17991> (accessed June 14, 2022).

(106) Stogiannidis, E.; Laane, R. Source Characterization of Polycyclic Aromatic Hydrocarbons by Using Their Molecular Indices: An Overview of Possibilities; **2015**; pp 49–133. DOI: 10.1007/978-3-319-10638-0_2.

(107) Qian, K.; Rodgers, R. P.; Hendrickson, C. L.; Emmett, M. R.; Marshall, A. G. Reading Chemical Fine Print: Resolution and Identification of 3000 Nitrogen-Containing Aromatic Compounds from a Single Electrospray Ionization Fourier Transform Ion Cyclotron Resonance Mass Spectrum of Heavy Petroleum Crude Oil. *Energy Fuels* **2001**, *15*, 492–498.

Recommended by ACS

Comprehensive Molecular Compositions and Origins of DB301 Crude Oil from Deep Strata, Tarim Basin, China

Meng Wang, Linxian Chi, *et al.*

MAY 01, 2020
ENERGY & FUELS

READ 

Carbazoles in Oils, and Their Application in Identifying Oil Filling Pathways in Eocene Syn-Rift Fault Blocks in the Dongpu Depression, Bohai Bay Basin, East China

Youjun Tang, Ting Wang, *et al.*

FEBRUARY 23, 2022
ACS OMEGA

READ 

Impact of Oil-Prone Sedimentary Organic Matter Quality and Hydrocarbon Generation on Source Rock Porosity: Artificial Thermal Maturation Approach

Amélie Cavelan, Fatima Laggoun-Déferge, *et al.*

JUNE 04, 2020
ACS OMEGA

READ 

Impact of Maturation on the Validity of Paleoenvironmental Indicators: Implication for Discrimination of Oil Genetic Types in Lacustrine Sha...

Hong Zhang, Mei Liu, *et al.*

MAY 12, 2020
ENERGY & FUELS

READ 

Get More Suggestions >